

Powering the Blue Economy - Ocean Observing Use Cases Report

February 2020

Andrea E Copping
Dale S Jenne
Yang Yang

Rebecca E Green
David M Greene

Robert J Cavagnaro
Jayson J Martinez

DISCLAIMER

This report was prepared as an account of work sponsored by an agency of the United States Government. Neither the United States Government nor any agency thereof, nor Battelle Memorial Institute, nor any of their employees, makes **any warranty, express or implied, or assumes any legal liability or responsibility for the accuracy, completeness, or usefulness of any information, apparatus, product, or process disclosed, or represents that its use would not infringe privately owned rights.** Reference herein to any specific commercial product, process, or service by trade name, trademark, manufacturer, or otherwise does not necessarily constitute or imply its endorsement, recommendation, or favoring by the United States Government or any agency thereof, or Battelle Memorial Institute. The views and opinions of authors expressed herein do not necessarily state or reflect those of the United States Government or any agency thereof.

PACIFIC NORTHWEST NATIONAL LABORATORY
operated by
BATTELLE
for the
UNITED STATES DEPARTMENT OF ENERGY
under Contract DE-AC05-76RL01830

Printed in the United States of America

Available to DOE and DOE contractors from the
Office of Scientific and Technical Information,
P.O. Box 62, Oak Ridge, TN 37831-0062;
ph: (865) 576-8401
fax: (865) 576-5728
email: reports@adonis.osti.gov

Available to the public from the National Technical Information Service
5301 Shawnee Rd., Alexandria, VA 22312
ph: (800) 553-NTIS (6847)
email: orders@ntis.gov <<https://www.ntis.gov/about>>
Online ordering: <http://www.ntis.gov>

Powering the Blue Economy - Ocean Observing Use Cases Report

February 2020

Andrea E Copping
Dale S Jenne
Yang Yang

Rebecca E Green
David M Greene

Robert J Cavagnaro
Jayson J Martinez

Prepared for
the U.S. Department of Energy
Under Contract DE-AC05-76RL01830

Pacific Northwest National Laboratory
Richland, Washington 99352

Executive Summary

The Blue Economy is an emerging sector that will require energy to allow many scientific, military, and commercial activities to reach their potential. With the publication of the DOE Water Power Technologies Office (WPTO) report “Powering the Blue Economy” (PBE), the first steps were taken in identifying and exploring the use of marine renewable energy (MRE) to power key blue economy end uses and applications. The applications or “markets” from the PBE report are divided into two major groups: Power at Sea, and Resilient Coastal Communities. Each market was analyzed in the PBE report with respect to overall size of the existing and potential market; MRE compatibility with functional requirements of existing technologies; competitive positioning with respect to other power sources; a reasonable path to market; and alignment to WPTO and other U.S. federal agency missions.

Among the end uses identified in the PBE Report within Power at Sea, ocean observing and autonomous underwater vehicle (AUV) recharge were considered to have potential as near-term markets for powering by marine energy. This identification of ocean observations and underwater recharge (from here on referred to simply as ocean observations) is based on the readiness of the existing ocean observations technologies, the high proportion of total project costs that is attributable to power needs, and the presence of partner organizations within the U.S. willing to engage with the national laboratories and WPTO on the topic.

Ocean Observation Use Cases

In order to explore the potential for MRE to power ocean observations and underwater recharge of AUVs, it is necessary to subdivide and specify the major types of ocean observations platforms, and to determine how each major type could be powered by MRE alone, or in conjunction with other renewable energy sources. Through a series of surveys and interviews with over 50 ocean observation experts and organizations, the two national laboratories categorized ocean observations platforms into stationary and mobile platforms, and further divided them by overall power needs. Five representative use cases were chosen among the many different types of ocean observation platforms in order to: 1) explore power needs that range from milliwatt scale to low-kilowatt scale for specific ocean observation platform types; 2) explore a variety of MRE resources coincident with specific ocean observation platforms including wave, tidal, ocean current, and thermal gradients; 3) develop a range of methods and tools for examining potential MRE resources and their coincidence with other potentially viable renewable energy sources; and 4) investigate common design solutions applicable across a range of disparate ocean observation platform types and which may be applicable for other Power at Sea applications.

The five use cases do not all represent existing ocean observation platforms; each is based loosely on an existing platform but several have been expanded in scope and design to address future ocean observation missions for future data collection and observation, expressed by the ocean observation experts. Each use case was located in a specific area of the ocean, to enable the most realistic estimates of renewable energy sources at that location and to match the power needs of the platform with the mission and constraints in that space. Additionally, all cases selected exhibit strong potential and existing or expressed willingness to partner on future activities.

Use Case Summaries

The use cases have been created by the two national labs to provide models for examining functional requirements, constraints and barriers, and engineering pathways for moving forward with research and development to supply power to ocean observation platforms. The process of developing the use cases, further delving into power requirements, design limitations, and

planning for bench scale design, build, and test of prototypes, will inform a range of potential MRE-powered Blue Economy markets. The investigations should also empower the MRE industry to advance technology development, testing, and demonstration, and will inform WPTO activities for advancing MRE deployments through SBIRs, FOAs, lab calls, prizes and challenges, and other funding mechanisms. The five use cases defined and analyzed by the two national laboratories are described here.

Use Case #1: Powering a High-Latitude Coastal Weather Buoy

Data from the National Oceanic and Atmospheric Administration (NOAA) National Data Buoy Center's (NDBC) weather buoys provide critical information for accurate weather forecasting, but the buoys can be power limited, especially at high latitudes where solar energy is low in winter, which restricts their data collection capacity. Power from waves is by far the strongest and most persistent at the Alaska site chosen for this case study (Shelikof Strait), compared to tidal, solar, and wind. A small wave energy converter (WEC) integrated with or near the buoy would be sufficient to provide the required power for integrated and enhanced sensing, increasing the sampling rate and communications frequencies, and reducing reliance on backup battery systems.

Use Case #2: Expanding High Frequency Radar for Resiliency in Coastal Communities

High frequency (HF) radar is used to inform a range of end uses, including U.S. Coast Guard search and rescue (SAR) operations, NOAA's emergency response to hazardous spills, and National Weather Service operations. However many coastal areas of the U.S. lack HF radar installations due to lack of sufficient reliable power. This use case is placed just offshore along one of the key shipping transit areas on the west side of Cook Inlet, Alaska, which has been identified as an important missing link in the Alaska Ocean Observing Systems (AOOS). No grid power is available at this remote location, but adequate tidal currents can provide sufficient power.

Use Case #3: Powering AUV Docking Stations

AUVs are dependent on battery power for missions and must return to surface ships or shore bases for recharge, creating enormous costs and inhibiting stealthy operation. The AUV industry has identified development of an AUV docking and recharging system as a clear goal for reducing mission costs and extending the range of applications across scientific, industry, and defense applications. This use case is placed on the Ocean Observatories Initiative (OOI) Coastal Pioneer array off the U.S. east coast (southwest of RI), where an active program of resident AUVs is providing critical science data. An AUV recharge docking station prototype has been tested at the site. There is plentiful power from waves in the area, which could be used to power a year-round docking system offshore.

Use Case #4: Powering Deep Ocean Tsunami Detection Stations

Deep ocean tsunami detection stations are critical for identifying undersea earthquakes that can trigger deadly tsunamis. The systems placed at depth and at the surface rely on battery power, which eventually need to be replaced; the addition of renewable sources could extend system life, reduce operational costs, and improve reliability of the warning system. A combination of renewable energy sources (wave and solar) are likely to provide the best power sources at the selected location off the coast of the northeastern U.S. More power would allow for longer intervals between maintenance visits, more powerful sensors, and improved system redundancy.

Use Case #5: Powering a Drifting Profiler

Drifting profilers, such as those making up the 4,000-strong Argo array, are an important

component of the global ocean observing system. If energy could be harnessed from the environment, the supplemental power available to the profiler could increase its operating life, enable higher sampling rates, and allow for the deployment of additional sensors. There are multiple potential sources of energy that could be extracted during the profiling portion of a mission, including thermal gradients, wave, current, and solar. Since drifting profilers need to operate throughout the world's oceans there may not be a one-size-fits-all approach to harvesting energy.

Evaluating Renewable Energy Resources

Consistent methods were used for characterizing renewable energy resources for the specific ocean locations whenever possible, using wind, waves, current, and irradiance measurements from ocean observation platforms. Locations for some of the use cases were selected in-part due to the availability of resource information. Simulations of tidal currents and solar irradiance were employed when direct measurements were not available. Open-source tools developed by the national labs were used to estimate solar and tidal power. MRE devices have been modeled in a simple manner to reduce complexity while still providing insight into the match of devices and energy resources needed to power the selected ocean observation platform.

Three sites were picked in the ocean for locations appropriate for use cases #1-#4; the renewable resources have been characterized at those sites. The fifth use case (profiling drifter) was treated differently as floats do not remain in a single location and are deployed in many locations throughout the oceans. A summary of resource results for the first four use cases is compiled in Table 1.

Table 1. Summary of available resources at use case locations.

Case(s)	Location	Wave (W/m)	Current (W/m ²)	Wind (W/m ²)	Solar (W/m ²)
1	Shelikof Strait, AK	4800	5.3	430	138
2	Cook Inlet, AK	120	361	107	250
3, 4	NW Atlantic Ocean	12400	11	298	162

Contents

Executive Summary	iv
1.0 Introduction	1
1.1 Background	1
1.2 Methods	2
2.0 Use Case #1: Powering a High Latitude Coastal Weather Buoy	3
2.1 Introduction and Value Proposition	3
2.2 Technology Description	4
2.2.1 Hull, Mooring, Deployment, and Recovery	4
2.2.2 Sensors	4
2.3 Cost Drivers	5
2.4 Energy Use	5
2.5 Resource Availability	6
2.5.1 Wave Power	6
2.5.2 Solar Power	7
2.5.3 Tidal Power	8
2.5.4 Wind Power	8
2.6 Potential Partners	8
2.7 Conclusions	9
3.0 Use Case #2: Expanding HF Radar for Resiliency in Coastal Communities	10
3.1 Introduction and Value Proposition	10
3.2 Technology Description	11
3.3 Cost Drivers	11
3.4 Energy Use	12
3.5 Resource Availability	12
3.5.1 Tidal Power	13
3.5.2 Solar Power	13
3.5.3 Wind Power	13
3.5.4 Wave Power	14
3.6 Potential Partners	15
3.7 Conclusions	15
4.0 Use Case #3: Powering AUV Docking Stations	16
4.1 Introduction and Value Proposition	16
4.2 Technology Description	17

4.2.1	Energy Conveyance and Storage	19
4.3	Cost Drivers	19
4.4	Energy Use	19
4.5	Resource Availability	19
4.5.1	Solar Power	20
4.5.2	Wind Power	20
4.5.3	Wave Power	21
4.5.4	Ocean Current Power	21
4.6	Potential Partners	22
4.7	Conclusions	22
5.0	Use Case #4: Powering Deep Ocean Tsunami Detection Stations	24
5.1	Introduction and Value Proposition	24
5.2	Technology Description	24
5.3	Cost Drivers	25
5.4	Energy Use	26
5.5	Resource Availability	26
5.6	Potential Partners	27
5.7	Conclusions	27
6.0	Use Case #5: Powering a Drifting Profiler	28
6.1	Introduction and Value Proposition	28
6.2	Technology Description	28
6.2.1	Argo Floats	29
6.3	Cost Drivers	31
6.4	Energy Use	32
6.5	Resource Availability	34
6.5.1	Thermal Power	34
6.5.2	Wave Power	36
6.5.3	Current Power	37
6.5.4	Solar Power	39
6.6	Potential Partners	40
6.7	Conclusions	41
7.0	Conclusion	42
Appendix A	Use Case Locations	A.1
Appendix B	Resource Characterization Methods	B.1
B.1	Wave Power Estimation	B.1

B.2 Tidal and Ocean Current Power Estimation B.1
B.3 Wind Power Estimation B.2
B.4 Solar Power Estimation B.2

Figures

1	SCOOP payload in foam discus buoy.	4
2	Bivariate distributions of sea states for time and energy at Station 46077.	7
3	Estimated output of an 800 W rated point absorber WEC.	7
4	Estimated solar power output for existing panel configuration.	8
5	Estimated wind power output for a 500 W rated horizontal axis wind turbine.	9
6	Example surface current speeds measured by HF radar off the U.S. West Coast.	10
7	CODAR Ocean Sensors SeaSonde HF radar system in California.	11
8	Estimated power output over many tidal cycles for a 1.5 kW rated tidal turbine.	13
9	Estimated power output for a 1.5 kW rated solar array.	14
10	Estimated power output for a 700 W rated horizontal axis wind turbine.	14
11	OOI Coastal Pioneer surface and subsurface assets with prototype AUV dock.	18
12	Estimated power output of existing solar array at surface mooring.	20
13	Estimated power output of existing wind generation units at surface mooring.	21
14	Bivariate distributions of sea states for time and energy.	22
15	Estimated output of a 2 kW rated point absorber WEC.	22
16	a) DART II system components (NDBC 2019a); b) NDBC tsunami station locations.	25
17	Components of DART II surface buoy (Meinig et al. 2005).	25
18	Map of current and planned Argo float deployment. a) Functional Argo floats, as of 12/15/2019, distributed throughout the world’s oceans (Courtesy of UCSD); b) Schematic of the Argo2020 design indicating the density of the 4600 floats targeted in the system design (Source: JCOMMOPS).	29
19	Example of Argo float and operation. a) Schematic of Argo SOLO-II float (Courtesy of Michael McClune at Scripps Institution of Oceanography); b) Park and profile mission operation (Courtesy of UCSD).	30
20	Schematic diagram of profiler motion in the sea (Xia et al. 2017).	35
21	a) A schematic of the Wirewalker vertical profiler. Vertical motion of the surface float is transferred to the weighted deployment wire and rectified by a cam in the profiler. b) Schematic of the Wirewalker cam during ascent and descent. (Pinkel et al. 2011)	37
22	3D drawing of profiling float with a characteristic diameter less than 0.4 meter and schematic diagram of the internal profile of the turbine connecting mechanism. (Wu, Liu, and An 2018)	38
23	Photo of the Teledyne Marine APEX Current Profiling Float which utilizes a vane ring to generate rotational motion during a profile, which is involved in a process of directly measuring water current using motionally-induced electric fields.	38
24	General size and location of the stability disk of an Argo float. a) Schematic of a SOLO float (Bishop et al. 2003); b) Photo of a PROVO float at the water surface	40
A.1	Locations of use cases #1 and 2.	A.1
A.2	Locations of use cases #3 and 4.	A.2

Tables

1	Summary of available resources at use case locations.	vi
2	SCOOP payload power and energy summary.	6
3	WHOI/OOI Docking System Power Draw.	20
4	Energy breakdown by components for a Teledyne Apex float with nitrate and oxygen sensors averaged over 374 profiles (Gordon 2017).	33

1.0 Introduction

1.1 Background

The PBE report published in Spring 2019 launched a new initiative within the Water Power Technologies Office of the same name. The goal of the initiative is to better understand the myriad non-grid markets that might benefit from marine energy integration through market analysis and targeted R&D. Within the PBE Report the ocean observing market, to include recharging of AUVs, scored relatively high with respect to market size, marine energy compatibility with functional requirements, competitive advantage over incumbent technologies, and alignment with DOE and other Federal Agency objectives. Due to these perceived advantages, a team of NREL and PNNL lab staff chose ocean observations and AUV recharge as a focus for its FY20 PBE AOP activities to support the PBE Initiative in its first year.

This report provides five real-world use cases that fall within ocean observing systems that might benefit from marine energy integration. These use cases are a first step towards understanding the value of marine energy for providing power, including descriptions of sensing technologies, cost drivers, energy use, resource availability, and the potential for partnerships in developing the use cases. In follow-on analyses for each use case, the two labs will define functional requirements, identify constraints and barriers to engineering design, and document design parameters for suitable MRE technologies to power the ocean observation use cases.

Building on information gathered for the Powering the Blue Economy Report, the use cases and information were informed by many interviews and surveys with ocean observing experts in academia, government, and industry, spanning a wide range of observing sensors, platforms, and marine environments. The use cases were selected based on the best value proposition for marine energy integration, end-user feedback, and their potential to enhance ocean observing missions.

The five use cases represent key examples of ocean observation systems around the world that are limited to varying degrees by power availability. They include: powering metocean buoys, profiling floats, tsunami warning stations, HF radars, and AUV recharge. For each use case the technology is described, cost and energy drivers are discussed, and suitable ocean energy resources evaluated.

A recent updated market size analysis presented by the lab team in October 2019 identified that the largest US PBE markets include ocean observing and AUV recharge, based on currently available data. The world market for navigational and survey instruments more than doubled between 2001 and 2011, with approximately 7% compound annual growth rate (CAGR) from \$7.5 billion to \$16 billion. Many of these instruments are used for ocean observation and navigation purposes, indicating a growing need for power at sea to supply these systems. AUV recharging has a variety of applications, especially in defense communities, with the U.S. holding the major market share for AUV production. Assuming that growth could be 10% CAGR, the AUV recharging market in the U.S. may grow from its current value of \$3 billion to \$8 billion by 2030.

Each use case is presented as a section within this report, consisting of subsections describing the energy value proposition, the specific ocean observation technology, the cost drivers, energy use by the ocean observation system, and characterization of the available renewable energy resource. The methods employed for estimating the available energy resources are described in the methods section of the report as there is considerable overlap among the cases. The most common renewable source that appears to meet the needs of ocean observation systems comes from ocean waves, followed by tidal and ocean currents, solar energy, wind energy, and gradients in ocean water including thermal and pressure

gradients.

1.2 Methods

The two national labs developed five use cases for ocean observing and AUV recharge to better understand the specific challenges for building and designing marine energy equipped systems for these applications. The specific use cases that might benefit from marine energy were identified and influenced using the outcome of an intensive set of interviews and surveys with ocean observing experts from academia, government, and industry, carried out during the spring and summer 2019 (Green et al. 2019). A follow-up interactive session to gather expert feedback from the ocean observing community was conducted by the lab team during the Oceans19 Conference in Seattle.

Use cases were chosen to include metocean buoys, profiling floats, tsunami warning stations, HF radars, and AUV recharge, all of which play an important role in ocean observation systems around the world. Each is limited in-part by power availability. The lab team carried out additional interviews to further hone each chosen use case, with key experts in the field, including those from NOAA, NDBC, Pacific Marine Environmental Laboratory (PMEL), University of Alaska Fairbanks (UAF), University of California San Diego (UCSD), CODAR, and Woods Hole Oceanographic Institution (WHOI). The experts provided feedback on the ocean observation technologies, cost drivers, energy use, resource availability, and potential for partnerships. Specific locations for each use case were identified based on the likelihood of marine energy providing a strong value proposition. At each location, a comparison of resource availability for renewable energy sources (including wave, marine current, solar, and wind) was performed. Detailed methods on estimation of each resource are provided in Appendix B.

Databases for marine energy resource intensity, such as the MHK Atlas, were found to be useful for identifying broad or regional potential. For specific deployment sites, data from measurement platforms will be necessary to attain the resolution required for accurate estimates of available power. Two of the selected use cases employ existing ocean and meteorological measurement packages, allowing direct characterization of resources. Other use cases were sited at or near similar stations, allowing the use of consistent methods. Where field measurements for resource characterization were not present, modeling methods were employed. Systems currently used to harvest energy on studied observation platforms are modeled. Hypothetical systems (e.g., wave energy converters) are all sized and modeled to achieve a capacity factor (ratio of average to rated power) of about 30% to maintain consistency across different resource types and intensities. A 30% capacity factor is common for sizing and rating components for the most likely conditions while recognizing the value of producing power during rarer, higher energy periods. Capacity factor is influenced by the power rating and size of the power system. Discretion was used to select the characteristic dimension (size) of hypothetical converters with goals of producing above and beyond the existing power requirements while maintaining scale of deployment similar to the existing infrastructure. For example, proposed wave devices were specified to not exceed the characteristic dimensions of the platforms they are powering to ensure deployment and recovery requirements are comparable to those for the existing hardware. Once size is established, power rating is solved for to attain the desired capacity factor. For first-order estimates of system performance, these methods are reasonable. However, actual system development will depend on the physical and electrical parameters of engineered components and may not result in idealized dimensions, ratings, or capacity factor.

2.0 Use Case #1: Powering a High Latitude Coastal Weather Buoy

2.1 Introduction and Value Proposition

NDBC operates a global network of assets to collect meteorological and oceanographic measurements. These data are made available as a public service and employed by a wide range of end users for forecasting weather, marine conditions, tracking of ocean properties, and many other services. Of these assets, there are 106 moored coastal weather buoys (CWBs) in the Northern Hemisphere. Nineteen stations are located in high latitudes above 50°N in the Gulf of Alaska and Bering Sea. These buoys face challenges due to their remoteness (difficulty and cost of servicing), harsh oceanic conditions, and lack of sunlight outside the summer months. The latter condition results in a power constraint for buoys employing solar panels. Due to the size of battery banks and limited generation capabilities, sensor payloads, duty cycles, onboard processing, and frequency of communications are all limited. There is an opportunity to enhance the capabilities of these systems by supplementing their solar panels with energy from waves or tides.

This use case reflects the findings of the PBE Report Chapter 2: Ocean Observation and Navigation. The report outlines a particular opportunity for systems and sensors operating continuously at high latitudes, utilizing marine energy combined with energy storage and other renewables. Increased power is anticipated to allow more power-hungry sensors, longer deployments, higher sampling rates, and enhanced outcomes for forecasts and navigation aid. The application of marine energy to this market is considered promising because of logical colocation benefits and its near-term needs and priorities.

Following the release of the PBE Report, the research team conducted surveys as well as phone and in-person interviews with ocean observations end users to refine and expand on limitations, desires, and opportunities for the integration of marine energy. Of the respondents contacted throughout this research, 32 discussed buoys, floats, or tags and 10 (with some overlap) discussed high latitude stations. Of specific interest were comments from NDBC representatives who listed power as a “monumental constraint”, forcing hard choices about sensors, communications, throughput, and onboard data processing. They note uncertainty in the functionality of new buoy payloads at high latitudes. They noted the high costs of servicing systems on a two year maintenance schedule, dwarfing the capital costs of the batteries currently used, which themselves might be replaced several times over a ten year operating life. When respondents were asked what they would do if they had greater amounts of power available, they listed avoiding ship time, having the ability to self-clean, enabling some form of propulsion, and allowing for sensor exchange as high priorities. Buoy system engineers listed additional prospects of enhanced data processing capabilities, video streams, biogeochemical sampling, radar, advanced automation, and continuous sonar.

The chosen CWB for this use case analysis is NDBC station 46077, located in Shelikof Strait, AK (NDBC 2019b). To the west of Kodiak Island and leading from the Aleutian Archipelago to Cook Inlet south of Anchorage, the strait is frequented by a local fishing fleet and sees transits of cargo and tanker ships. Sensors are currently limited to those providing simple atmospheric (e.g., wind speed, temperature) and oceanographic (e.g., wave height, temperature) data. However, more power-intensive sensors providing more detailed data including current speed and biogeochemical properties would be useful for improving forecasts. Cameras providing real-time video feeds could aid boats to observe sea states. Furthermore, additional power would enable the use of active biofouling mitigation methods, potentially extending intervals between servicing which are currently driven by the need to clean and recalibrate instruments.

2.2 Technology Description

NDBC weather buoys are in a period of transition to an updated technology platform, the Self-Contained Ocean Observations Payload (SCOOP), shown in Fig. 1. The last of the buoys to be transitioned are those above 48°N due to challenges in accessing high-latitude locales. The system is engineered to be deployed for two years, though are typically serviced every 12-18 months, allowing for some contingency time.

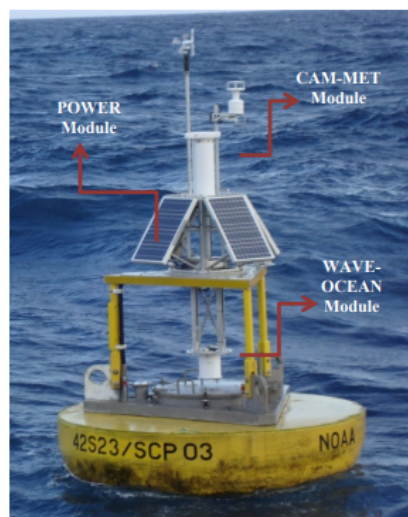


Figure 1. SCOOP payload in foam discus buoy.

2.2.1 Hull, Mooring, Deployment, and Recovery

SCOOP instrumentation and power system payloads are typically deployed on two to three-meter diameter aluminum or foam discus-shaped hulls. The sensor/power package is 90 kg and designed to be modular for integration with many buoy types. CWBs utilize slack moorings of steel chain and synthetic rope, anchored with concrete or steel weights. Each anchor has a surface area of 2.3 m², typically weighing around 3900 kg (NDBC 2018). The entire mooring system is not recovered during buoy recovery: the top section of line may be recovered, but the remaining components and anchors are left in location (NDBC 2018). CWBs are deployed and recovered from ships with appropriate lifting capabilities, either from stern A-frames or with cranes. Due to their mooring configuration, CWBs have a permissible watch-circle, or radius relative to their anchor position about which they may drift. Significant deviation from this watch-circle, as indicated by GPS, indicates a buoy has been disconnecting from its mooring.

2.2.2 Sensors

Sensor duty cycle of SCOOP instruments varies. Core sensor systems are a surface meteorology unit, data hub, automatic identification system (AIS) for ship traffic, camera package, subsurface ocean meteorology and wave package, and auxiliary package consisting of buoy-specific equipment that may be provided by third parties (Kohler, LeBlanc, and Elliott 2015). The surface meteorological package collects wind speed, direction, temperature, relative

humidity, atmospheric pressure, and compass heading data (Vaisala WXT-520, R.M. Young ResponseONE). The oceanographic package collects subsurface temperature or temperature and conductivity and may contain up to nine additional temperature, temperature and pressure, conductivity and temperature, or conductivity, temperature and pressure sensors or a thermistor array at different depths below the buoy (Kohler, LeBlanc, and Elliott 2015). These subsurface sensors transmit their measurements up the mooring line with an inductive modem. The wave system measures heave, pitch, roll, and direction. Each package communicates wirelessly to a central data, control, and communications hub, including a monitoring system for the power package. Data are transmitted on a ten-minute interval via the Iridium network (Iridium 9602 SBD modem). Camera data is transmitted wirelessly back-to-shore once per hour via satellite using an onboard 9522B Iridium RUDICS modem (Kohler, LeBlanc, and Elliott 2015).

2.3 Cost Drivers

Costs for equipment, operation, and maintenance are based on conversations with NDBC operations engineers and managers. They report the capital cost of a new SCOOP buoy to be \$200K, plus the cost of mooring equipment (anchor, line, hardware - cost variable with depth of deployment). Buoys are designed to survive without maintenance for two years, but are on a yearly maintenance cycle to keep sensors functioning, that can be stretched to 1.5 years if necessary. Maintenance scheduling is arranged such that several buoys within geographic proximity can be serviced during a single voyage. NDBC reports maintenance costs average \$60K per year per buoy, from vessel costs of \$20-25K per day, plus \$20K per service for personnel costs. This value does not include costs to replace broken equipment, which they note happens more frequently at high latitude stations due to harsh conditions. Costs may be increased due to emergency recovery operations when mooring failures lead to buoys going adrift.

2.4 Energy Use

NDBC operations engineers provided a breakdown of energy use for the SCOOP payload by subsystem. Energy use was provided in units of Ah (Table 2), with a nominal battery voltage of 10.8 V to determine daily average power draw.

The sensing platform, including data transmissions once every 10 minutes and photo transmissions once per hour uses very little power - averaging just 3 W continuous over a full day. Nearly one third of this power draw is reserved for third-party sensing. A heating system required to maintain the health of the SCOOP Li-ion rechargeable battery bank is enabled at 0°C and disabled at 3°C, doubling the average power draw in these conditions.

Power is generated from four 30 W solar PV panels mounted to the payload mast in a 90-deg. staggered configuration. This 120 W array feeds a 1.34 kWh Li-ion battery pack at a nominal voltage of 10.8 V. At the average power draw, 50% capacity of the battery bank would be expended after 14 days of operation with no additional energy input from the solar array. According to information provided by NDBC, subsystems can be toggled to reduce the electrical load, starting with any auxiliary packages, but maintaining wave and oceanographic payloads and data transmissions until only 10% of the battery capacity remains. Note the battery capacity does not include lithium primary batteries used for backup and to power the heating system if solar is insufficient.

Table 2. SCOOP payload power and energy summary.

Functional Module	Daily Energy (Ah)	Avg. Power (W)
Basic met. and oceanographic	0.55	0.25
Extended met. and oceanographic	0.17	0.08
Hub controller	0.41	0.19
Meteorological total	1.2	0.54
Waves	1.32	0.59
Ocean	0.03	0.01
Oceanographic total	1.35	0.61
Camera	1.97	0.89
AIS	0.003	0.001
Camera/AIS total	1.97	0.89
Aux. payload total	2.0	0.90
Battery heater	4.8	2.2
Total	11.3	5.1

2.5 Resource Availability

Due to the nature of the mission and capabilities of CWBs, they continually collect and report necessary data for characterizing the potential for wave and wind power generation. Tidal and solar power can be estimated using external tools.

2.5.1 Wave Power

Data from the studied asset are utilized to estimate the resource potential and expected output of a co-located or add-on WEC at the site. A bivariate distribution is shown in Fig. 2 for the full year of 2018. Most probable wave periods are between three and five seconds with heights between one-half and two meters. The average annual resource intensity is 4.8 kW/m, a value that would be considered low for electric utility grid applications, but likely sufficient for the given application.

For this use case, a characteristic dimension (diameter) of 1 m is chosen, resulting in an efficiency of 6.9%. Selecting a power rating of 800 W returns a capacity factor of 32% over the conditions of the 2018 buoy dataset. A time-series of estimated output is shown in Fig. 3. Average power output is estimated to be 254 W - two orders of magnitude higher than the average power consumption of the buoy in its current configuration. Note the weak power performance in winter months, consistent with low winds and typical for wave energy generation.

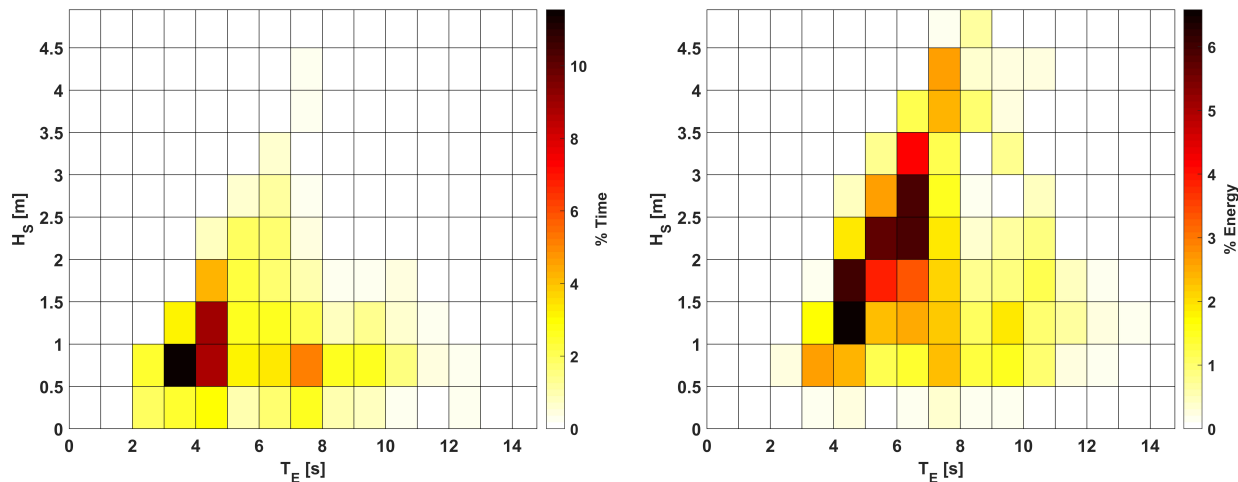


Figure 2. Bivariate distributions of sea states for time and energy at Station 46077.

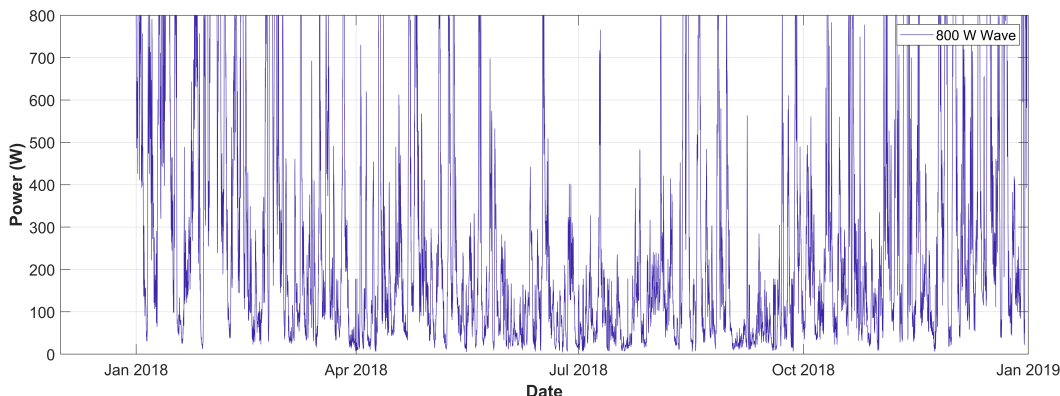


Figure 3. Estimated output of an 800 W rated point absorber WEC.

2.5.2 Solar Power

Both the current generation of CWBs and the newer SCOOP payloads utilize solar power from small panels mounted on the buoys. This power, replenishing a battery bank after an initial charge and with the potential for use of primary battery backups, is enough to maintain operation of a CWB at this location with current payload over a full year. Station 46077 is not equipped to measure insolation/irradiance, therefore estimates and simulation from other sources are used to gauge the resource.

NREL’s PVWatts tool is utilized to evaluate solar potential (Dobos 2014). Station 46077 is located 1.3 km from the center of a grid point for simulation. The buoy utilizes four 30 W panels each with estimated dimensions of 0.56 x 0.34 m, yielding a total area of 0.76 m². PVWatts simulation output for the year is shown in Fig. 4. Power is highest in spring and summer months, approaching the rated output of the panels during peak hours, and tapers off to very low output through winter. Average solar power for this configuration is estimated by PVWatts to be 14.3 W, from a resource intensity of 138 W/m².

These simulation results indicate the buoy would rely on stored energy in its battery bank to buffer through days during winter when average solar output would be insufficient to meet its

needs alone. The platform's control system allows subsystems to be shut down as the battery bank's state of charge decreases.

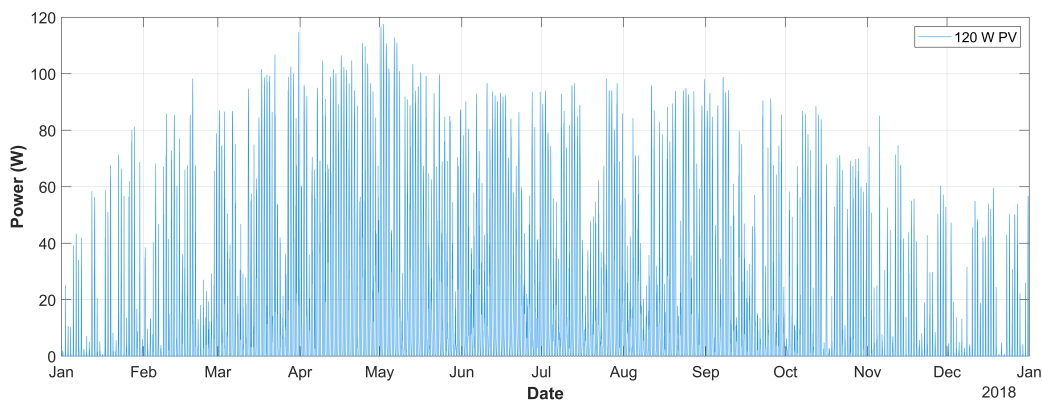


Figure 4. Estimated solar power output for existing panel configuration.

2.5.3 Tidal Power

Tidal currents were evaluated for the Shelikof Strait region over many tidal cycles and queried at the location of CWB 46077 to determine if there is sufficient resource to justify further investigation. Average speed simulated for the surface bin (closest to buoy deployment location) is 0.2 m/s, with a peak of 0.53 m/s, yielding an annual average kinetic power density of 5.3 W/m². Speed rarely rises above 0.5 m/s - lower than the cut-in speed for the vast majority of devices. Consequently, power output would be poor even if a suitable turbine is developed, yielding an average of just 0.1 W assuming a device with area of 1 m² and C_P of 0.3. Tidal energy is not viable for this location, but may be better suited for assets located in narrower tidal channels.

2.5.4 Wind Power

Buoy 46077 measures atmospheric conditions including wind speed and direction at a height of 4.9 m above the water surface. Average wind speed at the site is 7 m/s, with strong seasonal variation leading to powerful winds in the winter and weak winds in the summer. The yearly average kinetic power density for 2018 was 430 W/m². Assuming a wind turbine with 1.5 m² cross-sectional area (1.4 m diameter), a rated power of 500 W, and a C_P of 0.3, an average power over the year of 154 W is possible, yielding a capacity factor of 31%. This is 60% of the power output estimated for a WEC of smaller diameter. The result is intuitive, as waves represent a concentration of wind energy, which is itself a concentration of solar energy. A wind power time-series is shown in Fig. 5. The correlation to wave power is clear, as they exhibit the same short and long-scale temporal variation, indicating the sea state of the site is primarily driven by local winds.

2.6 Potential Partners

NOAA NDBC has provided feedback and information for this use case, including completion of surveys, in-person interviews, and furnishing of specifications and publications. Buoy

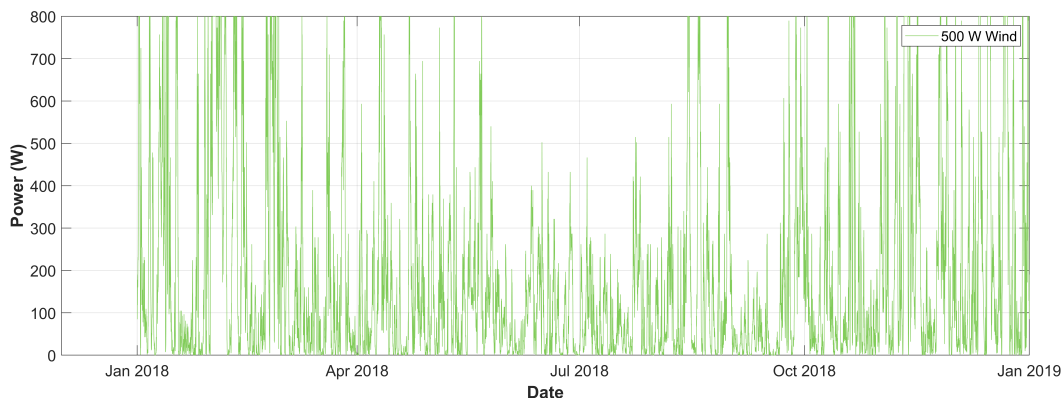


Figure 5. Estimated wind power output for a 500 W rated horizontal axis wind turbine.

measurement data, used to characterize the wave and wind resources at the deployment location, was acquired from NDBC's website.

2.7 Conclusions

NOAA CWBs serve a critical role for measuring ocean properties and informing forecasts. They have been engineered to use, on average, a very small amount of power by limiting their sensor suite and duty cycle. A new iteration of the buoy payload with more frequent transmissions will soon be deployed in the high-latitude region, including the station analyzed in this use case. Power from waves is by far the strongest and most persistent at the site, compared to tidal, solar, and wind. Should there be desire to integrate higher power sensing, increase sampling and communications frequencies, and limit reliance on backup battery systems, a small WEC integrated with or near the buoy would be sufficient to provide the required power. A combined wave and solar or wind and solar solution may be ideal due to the complementary seasonality of the resources.

Though this use case focused on a single location, it is anticipated that the conclusions are valid for most high latitude locations. Given the station's location in a strait, it is somewhat protected from higher waves expected in the open-ocean. Indeed, other locations are likely to have a stronger wave resource.

3.0 Use Case #2: Expanding HF Radar for Resiliency in Coastal Communities

3.1 Introduction and Value Proposition

High frequency (HF) radar systems measure the speed and direction of ocean surface currents in near real time. They can measure coastal ocean currents from a few kilometers offshore out to about 200 km, and are the only sensors that can measure large areas at the level of detail that is required for end users (Fig. 6). The radars are utilized to inform a range of end uses. For example, measurements of ocean currents inform understanding of coastal research and management (e.g., water quality monitoring), with both ecological and economic implications, as well as U.S. Coast Guard (USCG) search and rescue (SAR) operations, NOAA's Emergency Response Division's clean up of hazardous spills, and National Weather Service operations. HF radar is especially important to the resiliency of coastal communities, by providing coastal intelligence and allowing coastal communities to prepare for and react to long-term and immediate risks.

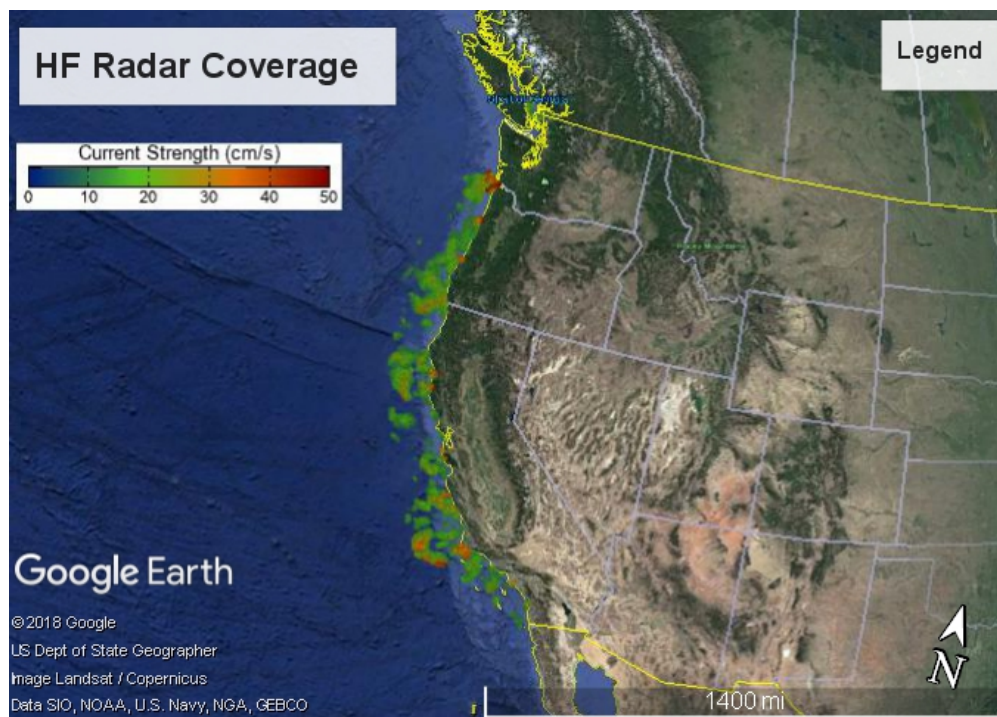


Figure 6. Example surface current speeds measured by HF radar off the U.S. West Coast.

Coastal HF radar surface current observations have been demonstrated to reduce USCG search areas when rescuing disabled vessels and people stranded in the water. The costs associated with SAR operations have been roughly estimated (O'Donnell and Pettigrew 2008). Multiple ocean observing experts interviewed indicated the desire for more power options to extend the geographic coverage of the current HF radar network, especially as many locations where the presence of HF radar would be very desirable are remote, and in comparison to other ocean observation platforms, the devices have high power needs. The U.S. IOOS operates the world's largest HF radar network made up of approximately 140 sites in nearly every coastal state and Puerto Rico. However, IOOS has identified critical location gaps where

HF radar still needs to be deployed to provide adequate coastal coverage (O'Donnell and Pettigrew 2008). For example, IOOS has identified as one of its priorities the deployment of new HF radars in remote locations (e.g., Alaska), which will require renewable and/or energy storage to operate, since many of these locations are off the grid. Interest was also expressed by interviewees in establishing offshore repeater stations for HF radar which would boost the signal out to greater distances from shore, beyond the current 200 km limit.

This case study will focus on the use of marine energy to power a new HF radar location in Alaska at one of the sites prioritized by the Alaska Ocean Observing System (AOOS). In its "Proposal for FY2016-2020 Implementation and Development of Regional Coastal Ocean Observing System" (Riemer 2015), key shipping transit areas were identified as being of high interest for new radars, including the Bering Strait, Unimak Pass in the Aleutian Islands, and Cook Inlet. There may be other locations for consideration, such as along the Oregon and Washington coast, Great Lakes, or Puerto Rico.

3.2 Technology Description

HF radar systems measure surface ocean currents by emitting radio waves from shore-based transmitting antennas. The radio waves are scattered by the ocean surface and part of the scattered energy returns to a receiving antenna (Fig. 7). Each station consists of a transmitter, receiver, one or two antennae (dependent on frequency), and a data acquisition/processing computer.



Figure 7. CODAR Ocean Sensors SeaSonde HF radar system in California.

The CODAR (Coastal Ocean Dynamics Applications Radar) SeaSonde is commonly used for this application and operates in standard, high-resolution, and long-range modes, each with an associated range resolution and frequencies (CODAR 2019b). HF radio formally spans the band 3-30 MHz. For CODARs, the upper limit is extended to 50 MHz. A vertically-polarized HF signal is propagated at the electrically conductive ocean water surface and can travel well beyond the line-of-sight, beyond which point more common microwave radars become blind. Rain or fog does not affect HF signals. Example equipment dimensions for a standard-configuration CODAR SeaSonde are: transmit antenna height of 4.8 m (for 11-14 MHz), transmit antenna post of 4 m, and receive antenna system of about 7 m, with receive and transmit chassis specifications also available from the manufacturer.

3.3 Cost Drivers

Capital costs for an HF radar system are roughly in the range of \$100K - \$200K. The manufacturer recommends maintenance intervals of every 6 months for visual inspection,

collection of archived data, and system calibration. Annual service visits are required at a minimum. University of Alaska Fairbanks (UAF) investigators have learned over time that the expense of logistics (e.g., helicopter) associated with resupplying propane or diesel fuel for generators results in unsustainable costs for operating remote HF radar sites. Vessel charters can deliver fuel at lower costs throughout Alaska, particularly in more accessible areas like Cook Inlet. However, inclement weather can hamper this form of delivery. Once the site is up and running, maintenance costs are minimal in comparison to the initial installation.

3.4 Energy Use

The CODAR SeaSonde power requirements are either 120 VAC or 220 VAC, 50-60 Hz; total onsite electronics varies between 350 and 500 W depending upon peripherals desired (CODAR 2019a). CODAR Ocean Sensors is now manufacturing a “low-power” SeaSonde unit powered by 24 VDC with 110/220 VAC external power supply, with a power consumption of 300 W peak and less than 150 W average (transceiver only and excluding any site accessories). The low power spec for power consumption includes cooling where the standard one does not include cooling. Cooling requirements will depend on installation location.

UAF is currently operating HF radar systems that are powered by renewable energy in northern Alaska (Point Barrow and Cape Simpson) using their modular, autonomous remote power module (RPM). Within the next year, they will also transition one of their two Bering Strait sites to off-grid renewable power, and they are re-installing their RPM system in Antarctica near the U.S. Palmer Station. The basic RPM system that UAF uses is described in (Statscewich et al. 2011). The subsystems are powered by a battery bank (with a five-day power reserve), charged primarily by wind and solar energy, and secondarily by a biodiesel generator on the Arctic coast. Recent experience indicates that the biodiesel generator is not necessary as wind energy is adequate to recharge the battery bank. The RPM supplies the daily power requirements of 7.5 kWh/day of a typical CODAR Ocean Sensors SeaSonde, a high-speed satellite communications link, a small meteorological station, and power monitoring and control equipment.

3.5 Resource Availability

Marine energy will have to be competitive with other renewable energy sources (solar and wind) to prove feasible for enabling an HF radar use case, with marine energy likely part of a hybrid renewable energy system. Unimak Pass has very high tidal currents which can flow through the Pass at more than five knots and may serve as a good source of marine energy. Other coastal Alaskan locations which have been prioritized for HF radar similarly have high tidal flows. For example, Cook Inlet is as an ideal location for tidal power, especially in locations where Alaska’s mountainous coastline would shelter a site from viable wind and solar resources. The eastern side of Cook Inlet is on the road system, but the western side is largely uninhabited and any deployments would require an islanded power system or microgrid.

A good candidate site in Cook Inlet is the Christy Lee Platform (Station DRFA2) located at Drift River Terminal, AK (NDBC 2019c). This meteorological station is located on a platform that was used for transferring oil from a holding area on the west side of the inlet to tankers that transport it to the other side. The holding station is being decommissioned, so there will be a lot of activity and boat traffic to the site in the near future (The Associated Press 2018).

Strategically, this is a good place to have HF radar coverage, and it is in a location where strong tidal currents exist. Furthermore, a turbine could be mounted directly onto the existing platform

to reduce capital expenditures. Two sites are needed for a full set of HF radar surface currents. A location across the inlet such as the town of Nikiski could serve as a suitable second location, either as a remotely powered site or connected to the grid if an appropriate site can be found.

3.5.1 Tidal Power

Tidal currents were evaluated in Cook Inlet using a Finite Volume Coastal Ocean Model (FVCOM) simulation over many tidal cycles and queried at the location of Station DRFA2. Current magnitude of the surface layer is used to estimate kinetic power density and the power output of a tidal turbine of 5 m² projected area (2.5 m diameter) with an overall system efficiency of 0.3, cut-in speed of 0.8 m/s, and rated power of 1.5 kW, sized to achieve a capacity factor of 29%. Resource intensity averaged over the year is 361 W/m². A time-series of tidal power output is shown in Fig. 8. Power is estimated at 439 W over many tidal cycles for the period of 2005 modeled. This result is expected to be typical over a full year. Of note are the periodicity and predictability of the tidal resource. However, there are phases of the tidal cycle during neap tide where speed is expected to be below specified cut-in for the turbine. Periodic intermittency necessitates the use of a battery bank.

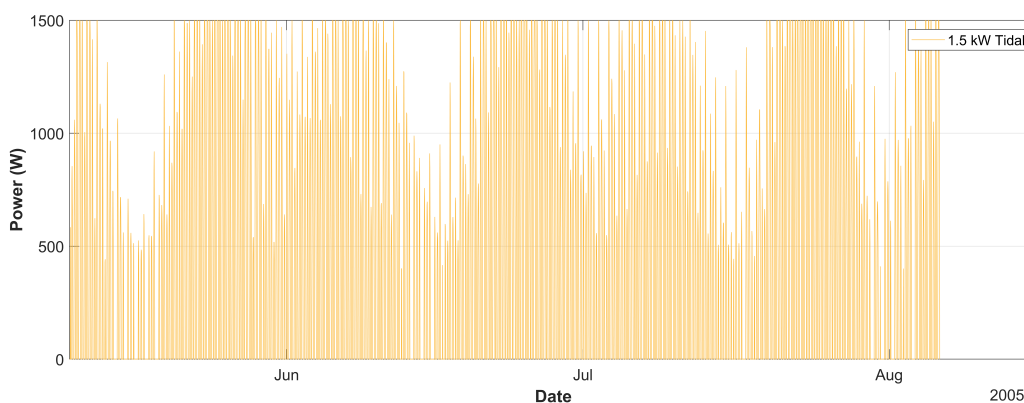


Figure 8. Estimated power output over many tidal cycles for a 1.5 kW rated tidal turbine.

3.5.2 Solar Power

Many NDBC meteorology platforms use solar power, but it is unclear whether or not Station DRFA2 follows suit. However, it is evaluated as an option for this use case. NREL's PVWatts tool is utilized to simulate a year of hourly-resolved solar output for a system rated for 1.5 kW, equal to the rating of the modeled tidal system. The station is roughly 64 km removed from the simulation node. The conditions for solar power are assumed to be relatively consistent over this range in the interior of Cook Inlet. A solar array of this size is estimated to average 161 W over a full year from a resource of 250 W/m². A time-series of output is shown in Fig. 9.

3.5.3 Wind Power

Station DRFA2 collects wind speed and direction data, utilized to estimate the output of a wind turbine mounted to the platform. Data from 2005 is selected to temporally match simulation output of tidal energy at the site. A device of 10 m² projected area (3.6 m diameter), an overall

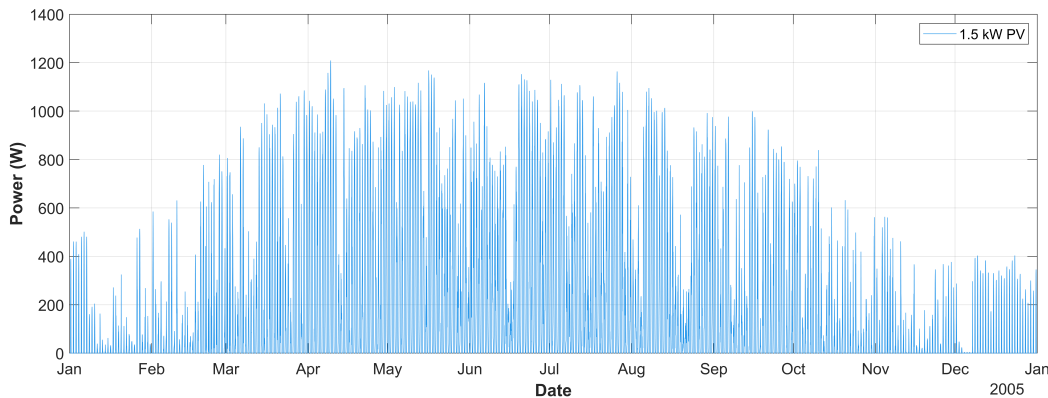


Figure 9. Estimated power output for a 1.5 kW rated solar array.

system efficiency of 0.3, and rated power of 700 W is modeled to reach a capacity factor of 30%. Estimated power output is shown in Fig. 10. Power is intermittent and inconsistent at the site, with an average kinetic power density of 107 W/m² and the modeled turbine averaging 209 W over the full year. Requiring a much larger wind turbine to attain similar power output and capacity factor as a tidal turbine is to be expected for a wind system, given the differences in density of the working fluid. However, the stochastic nature of the wind resource and long stretches of low power output would require a larger battery bank and more complex energy management system than for tidal.

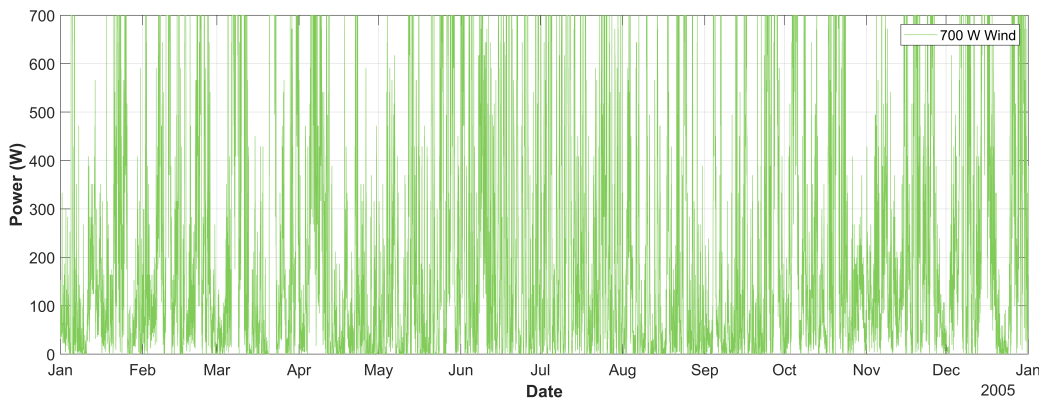


Figure 10. Estimated power output for a 700 W rated horizontal axis wind turbine.

3.5.4 Wave Power

Given the low wind resource and inland water location of this use case, wave power is not anticipated to be a viable resource. Additionally, no assets measuring sea state were identified in close proximity to the site. However, modeling results for Cook Inlet have been published in the NREL MHK Atlas (NREL 2019). The closest simulation node, several km from the station, averages 0.12 kW/m over a full year. Considering expected efficiencies of small WECs of less than 10%, this level of power would not be suitable for development.

3.6 Potential Partners

Potential partners who have indicated interest in this project include UAF College of Fisheries and Ocean Sciences and CODAR staff. Key staff within each of these organizations have contributed to the development of this use case and indicated interest in the possible application of marine energy towards extending the mission of HF radar systems. As this use case moves forward, these partners will be asked to assist with design elements for marine energy devices that will help connect marine energy power sources to HF radar stations without disrupting the essential mission of the platforms.

3.7 Conclusions

HF radar systems have tremendous societal and economic value by saving lives and property, such as through USCG SAR operations. If *in-situ* power were available, gaps could be filled in the current HF radar network in certain remote locations. Even in those places with wind or solar resource, the stochastic nature of these resources and potentially long stretches of low power output would require a larger battery bank and more complex energy management system. The selected site identified by this use case would be well suited to pair with tidal energy given the high power needs of a CODAR system and existing offshore infrastructure.

4.0 Use Case #3: Powering AUV Docking Stations

4.1 Introduction and Value Proposition

Autonomous underwater vehicles (AUVs) perform underwater tasks without a tether or line to a surface ship, carrying instruments and sensors to monitor, inspect, or otherwise interact with underwater environments making decisions using an onboard computer based upon external stimuli. The power capacity of an AUV's onboard battery limits its mission range and duration.

Underwater docking stations can theoretically expand the scope and duration of AUV missions by:

- recharging AUV batteries without recovering the vehicle on the surface,
- facilitating data transfer and increasing mission data storage capacity,
- maintaining a 'resident' presence for near-continuous observations,
- avoiding any surface presence apart from a possible communications node, and
- providing a secure platform to dock vehicles between missions and streamline vehicle deployment and recovery, among other possible benefits.

All of the above advantages could potentially be realized with a docking station cabled from shore, but the industry's available record shows no evidence of a successful, sustained operation of an AUV docking system: pilot projects have been conducted, but to our knowledge there is no established commercially available system at this time (Blue Logic launched its Subsea Docking Station product in September 2019, so it is too soon to independently assess its performance [Blue Logic 2019].) Engineering challenges around the control of the AUV to contact the dock (Fan et al. 2019), design of the mating interface, and control of the mating cycle – including even the ability to 'sleep' the AUV to avoid continuous power draw – have not yet been resolved but are surmountable. Incorporating a wave energy converter with a docking station cabled to shore does not appear to have been considered and does not appear to offer any advantages.

The added innovation of an uncabled, autonomously-powered docking station would provide additional benefits of increasing the geographic range (i.e., distance from shore) of possible locations. Incorporating a wave energy converter as a power source to complement the autonomous power source (e.g., wind or solar PV) would potentially extend the seasonal operability as well as provide redundancy in case of component failures.

Using a WEC as the sole source of power for an autonomous docking system is also a potential design; this could potentially minimize or eliminate altogether any surface expression of the system, which could be desirable for defense applications, although the lack of surface expression could inhibit communication modes that don't work underwater. Such a system is not the focus of this use case.

This use case explores the scenario of using supplemental wave energy to facilitate a docking system located far offshore and operated year-round. Such a system could have a range of potential applications including ocean observation, structural inspections, or even resource extraction based around a single docking station; or a network of such docking stations could conceivably allow extended missions from one station to another, much like a network of electric vehicle charging stations allows travel unconstrained by the onboard storage capacity.

One specific application of a docking system is the real-time monitoring of hurricanes. A docked and charged AUV could be pre-deployed in hurricane prone areas and lie in wait for

approaching storms. Once a storm develops, the AUV could be deployed rapidly without ever risking a ship and crew. The AUV could continue its mission by running multiple sorties from a single dock or by moving through a network of docks to follow the storm.

There are a number of challenges associated with powering AUV docking stations with marine renewables. One of the biggest challenges is integrating the marine energy system into the charging system that would be used for the AUV. Wave energy converters are located at or near the water surface where most of the energy is, however docking stations are typically located lower in the water column or on the seafloor. Putting charging stations on the seabed makes it easier for the AUV to dock by providing a stable platform, however getting power to the docking station is a non-trivial technical challenge.

4.2 Technology Description

This use case is challenged by the absence of any established commercial docking system, cabled or autonomous, on which to base proposed changes. In the absence of such an established platform, we will use the recently-piloted high powered mooring and AUV dock system developed by WHOI and deployed on the OOI Coastal Pioneer Array, shown in Fig. 11, as the base design.

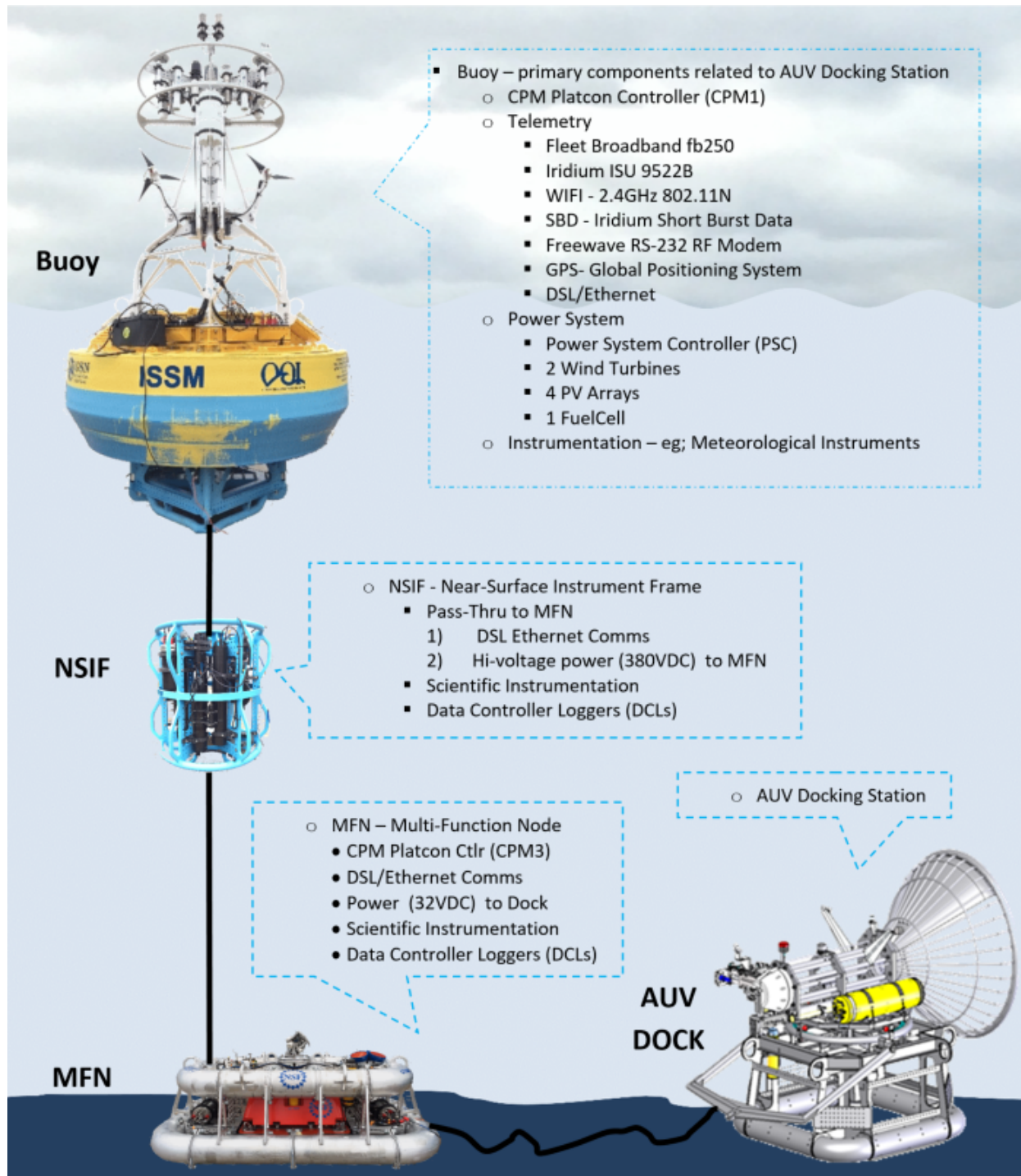


Figure 11. OOI Coastal Pioneer surface and subsurface assets with prototype AUV dock.

4.2.1 Energy Conveyance and Storage

The WHOI system provides power to the docking system by means of a 600 W 24 V to 380 V DC-DC power converter on the mooring, which supplies high voltage power for efficient transmission to loads on the Multi-Function Node (MFN) which is located on the seafloor. The MFN includes a power electronics assembly (MPEA) that provides DC-DC conversion of the high voltage power transmitted over the cable to low voltage (32 V) power for local MFN instrument loads and the AUV docking station. The surface mooring above AUV/dock includes a rechargeable 20 kWh (1667 Ah) marine lead acid battery bank.

4.3 Cost Drivers

Capital costs associated with the use case of providing power to a docking station are difficult to estimate due to the nature of the systems as prototypes. However, outreach to engineers of the OOI docking system revealed the operational cost to deploy their prototype charging system was about \$50K per day, while the cost to tend to an AUV (i.e., deploy, track, recover) is about \$15K per day. AUVs without docking stations require daily crewed activities. Assuming the same mission frequency planned for the docking station of 2 days of deployment per 5 days of charging, total mission operation costs of \$1.56M per year may be avoided by eliminating the need for operators. Additionally, vehicles customized to interface with the docking station were more expensive than standard units, at \$1.5M per unit.

Costs of the OOI surface mooring power generation assets are publicly accessible and summarized here. Capital costs (panels, mounting assemblies, and hardware) for the solar power system are \$10K per installed kW. For the wind system, costs (turbines, mounting assemblies, and hardware) are \$6.3K per installed kW. Battery costs including a mounting assembly are \$8 per Ah. For the deployed system, the capital costs for energy conversion and storage total about \$25K.

4.4 Energy Use

Power loads include platform hotel loads, instruments, and the AUV Dock. Loads would be managed according to different power management strategies for different operating modes involving the dock (idle, startup, charging). Specific loads, provided by WHOI through personal communications, are summarized in Table 3. The vehicle used with this prototype docking system is a Kongsberg REMUS 600 which includes a single or optional second 5.4 kWh Li-ion battery pack for a listed duration of 24 hours, subject to specific mission parameters and sensors (Kongsberg 2019).

4.5 Resource Availability

Resident AUVs are likely to be useful anywhere in the ocean, and the resources available to power a docking station will vary greatly. For the purposes of this use case, we select the location of the OOI Coastal Pioneer array, as it is the spot where a docking station prototype was originally tested and where there is an active program of autonomous vehicle operations returning critical science data. Nearby meteorological and oceanographic data is available from the OOI web portal. The Central Surface Mooring (CP01CNSM) is located 130 km offshore southwest of Block Island, RI, and is configured to collect wave motion, solar irradiance, surface current, and wind velocity, amongst many other properties (OOI 2019). These measurements

Table 3. WHOI/OOI Docking System Power Draw.

Specific Load	Power (W)	State of Charge / Hour (%)
Platform average power without dock	100	-0.5
AUV dock charging including efficiency	400	-2.0
Telemetry (standby)	20	-0.1
Telemetry (transmitting)	50	-0.25
Total	550	-2.75

are used to model and estimate the system’s current power generation profile and estimate the potential for marine energy. Solar, wind, wave, and ocean current power are considered.

4.5.1 Solar Power

Moored platforms in the Coastal Pioneer array are equipped with four 140 W-rated solar PV panels of 1 m² surface area each. Net shortwave irradiance averaging 162 W/m² over the year of 2017 is measured at the platform and serves as the resource data. Utilizing the methods described above to estimate PV performance through the PVLIB and SAM tools and a standard panel loss factor of 14%, a yearly average system output of 86 W is estimated. A time-series of output is shown in Fig. 12. Power output peaks during Spring and Summer and is limited between November and March. Available surface area for increasing the size of the PV system is limited on the existing OOI surface asset: additional panels would need to be on a separate platform if used and affect buoy windage and mooring.

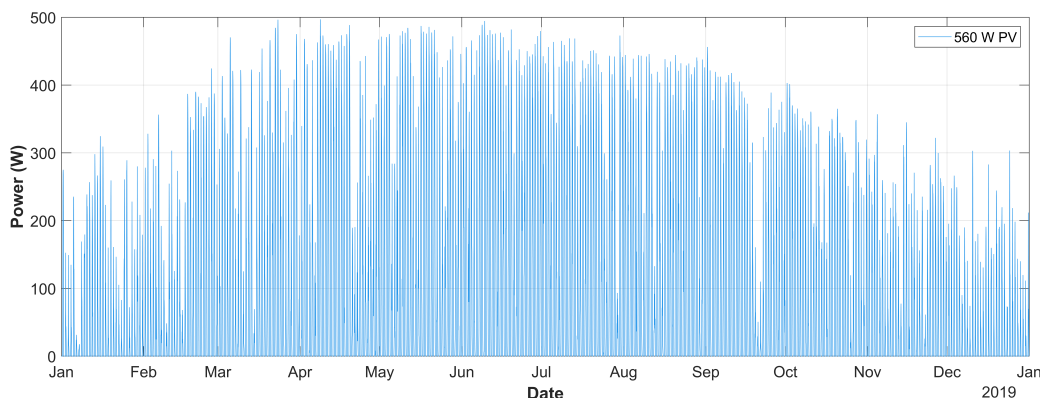


Figure 12. Estimated power output of existing solar array at surface mooring.

4.5.2 Wind Power

Two wind turbines provide power to the surface platform, mounted several meters above the ocean’s surface on the buoy’s instrumentation mast. Each turbine is 1.2 m in diameter, resulting

in a total of 2.3 m² projected area, and nominally rated for 350 W at 12.5 m/s for a coefficient of performance of 0.25. Assumed additional losses of 14% are applied, as for the solar case, for a total efficiency of 22%. Wind speed is collected with an ultrasonic anemometer just above the turbines on the instrumentation mast. The turbines' combined rated power at this location yields a capacity factor of 20%. An estimate of the system's wind power output is shown in Fig. 13. Average power for the system is 141 W over the full year from a resource with average kinetic power density of 298 W/m², with higher power output in winter. Note the period of sustained high winds in late September (and concurrent drop in solar power as seen in Fig. 12), corresponding to the remnants of Hurricane Jose.

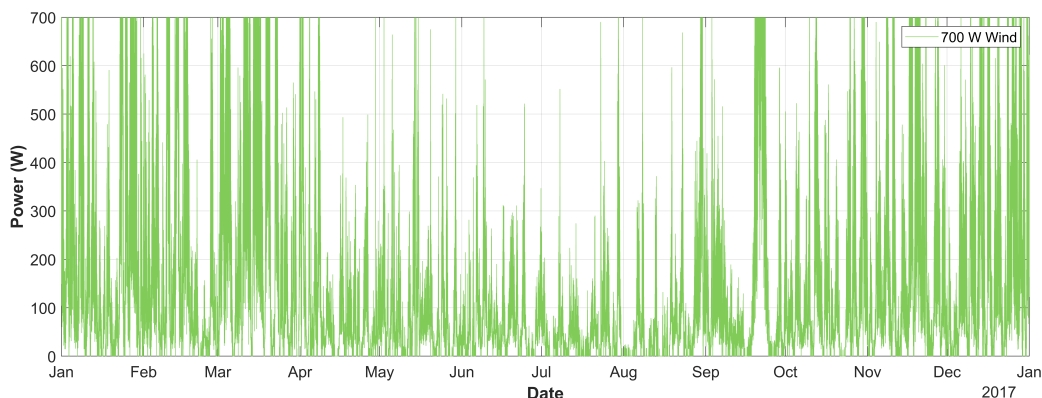


Figure 13. Estimated power output of existing wind generation units at surface mooring.

4.5.3 Wave Power

The quality and nature of the wave energy resource of the site is represented with a bivariate distribution, depicting significant wave height and energy period combinations as percentages of total time and energy (Fig. 14). Resource intensity at the site is 12.4 kW/m averaged over the year, indicating moderate potential for commercial development. Applying an efficiency derived for a 1 m diameter point absorber WEC of 6% and an additional balance of system efficiency of 86% and rating of 2 kW yields an estimated useable output averaging 621 W over the year. These conditions equate to a capacity factor of 31%. A time-series of this estimated output is shown in Fig. 15. Similar to wind, power performance is severely curtailed in the summer.

4.5.4 Ocean Current Power

Measurements of near-surface water current (7 m below surface) are collected by the platform using a single-point Doppler acoustic transducer. These are used to evaluate the location's potential for power generation from ocean currents. Average yearly kinetic power density is 11 W/m², and currents only exceed a presumed turbine cut-in speed of 0.8 m/s a handful of times over the year, yielding an average extractable resource of less than 1 W/m². Therefore, ocean current power is deemed not viable at this location.

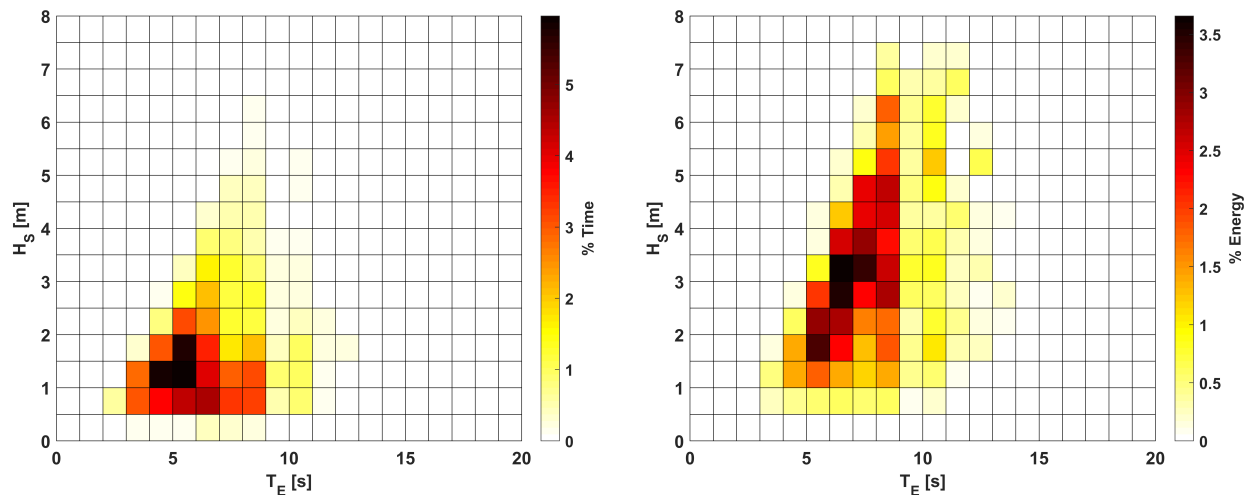


Figure 14. Bivariate distributions of sea states for time and energy.

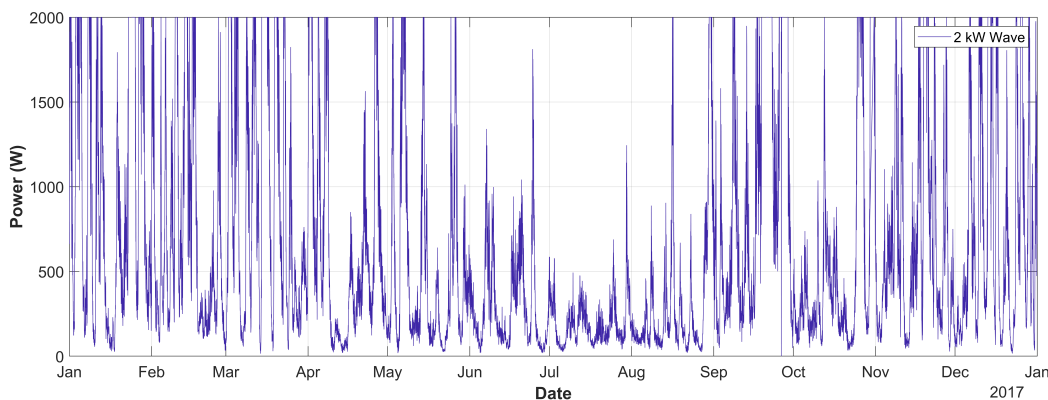


Figure 15. Estimated output of a 2 kW rated point absorber WEC.

4.6 Potential Partners

WHOI and other core OOI organizations are strong potential partners; their engineer indicated they would welcome further exploration of this idea. Monterey Bay Aquarium Research Institute (MBARI) has indicated equal interest in developing docking systems (MBARI 2019). SAAB has recently demonstrated a prototype docking system for their Sabertooth AUV and would be a potential industry partner (Maslin 2019).

4.7 Conclusions

Supplementing the WHOI system with a WEC to complement existing generation sources could enable year-round AUV operation by providing more power than similarly-sized wind turbines. This may translate to reduced operational costs for chartering ship time, fewer interventions, plus improved dataset quality. The AUV industry has identified development of an AUV docking and recharging system as a clear goal for reducing mission costs and extending the range of applications. Limitations to adaptation exist, in the form of a lack of standardization in AUV

power systems and continued challenges and requirements for biofouling and sensor calibration. However, the size of the market and importance of AUV missions for both scientific and defense applications makes this use case one of the strongest.

5.0 Use Case #4: Powering Deep Ocean Tsunami Detection Stations

5.1 Introduction and Value Proposition

Deep ocean tsunami detection stations are critical for identifying undersea earthquakes that can trigger deadly tsunamis (Bernard and Meinig 2011). These deep ocean stations are part of the larger tsunami warning system which both detects tsunamis and issues warnings to prevent loss of life and damage to property. Since 1850 alone, tsunamis have been responsible for the loss of more than 430,000 lives. The ability to detect potential tsunamis and initiate communications as quickly as possible is critical to minimizing these potentially devastating impacts. To this end, over the last thirty years, NOAA has developed the Deep-ocean Assessment and Reporting of Tsunami (DART) program, consisting of a real-time monitoring system that provides data for forecasting tsunamis. The National Data Buoy Center (NDBC) maintains and operates NOAA's DART systems which have been deployed in earthquake prone areas throughout the ocean. The DART system combines a surface buoy and a sensor on the ocean floor, which detects changes in water pressure, due to tsunamis, seismic waves or other pressure-impulse phenomena, and transmits the data back to the surface (Fig. 16a). If these changes indicate a tsunami may form, the buoy signals an alert via satellite to Tsunami Warning Centers onshore, such as in Alaska and Hawaii.

The high-level goal of this use case is to reduce operational costs and improve reliability of the warning system. Marine energy could provide an *in-situ* source of power to the DART buoys, which would allow for increased data collection, greater onboard processing, and faster communications, as well as longer ship-based maintenance intervals. This marine energy use case will focus on powering one of the DART surface buoys using wave energy at an Atlantic station off the U.S. East coast (Fig. 16b). The surface buoy has been chosen for this use case, because it stays out for less time (one to two years) than the seafloor package (two to four years) and thus requires more frequent ship-based maintenance. Additionally, the surface buoy is only used for communications, so there is little concern related to *in-situ* energy generation interfering with measurements.

5.2 Technology Description

NOAA PMEL developed the DART systems and has now evolved the DART II system, which incorporates the latest technologies and advances, have longer maintenance intervals, and feature two-way communication (Meinig et al. 2005). Detailed descriptions of the DART II system have been provided by NOAA (Fig. 17). The system is composed of two physical components, including a tsunameter on the ocean floor and a surface buoy with satellite telecommunications. The surface buoy has bi-directional communication links and are thus able to send and receive data from the Tsunami Warning Center and other operators. The surface buoy will be described in greatest detail here since it is the focus of this use case.

The DART II surface buoy is solely used for communications, relaying information and commands between the tsunameter and satellite network. The surface mooring uses a 2.5-2.6 m diameter fiberglass-over-foam disk buoy and 19 mm nylon mooring line, which keeps the buoy positioned within the cone of the acoustic transmission from the tsunameter. The buoy houses the following components: a modem and acoustic transducer, computer, Iridium satellite network transceiver, GPS, and batteries.

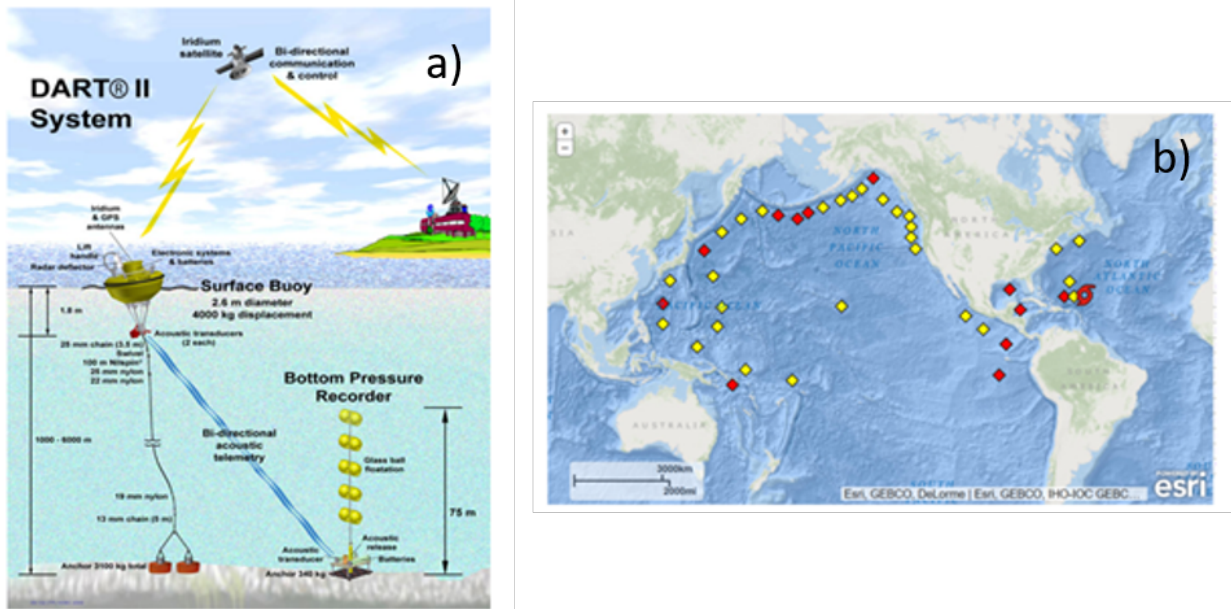


Figure 16. a) DART II system components (NDBC 2019a); b) NDBC tsunami station locations.

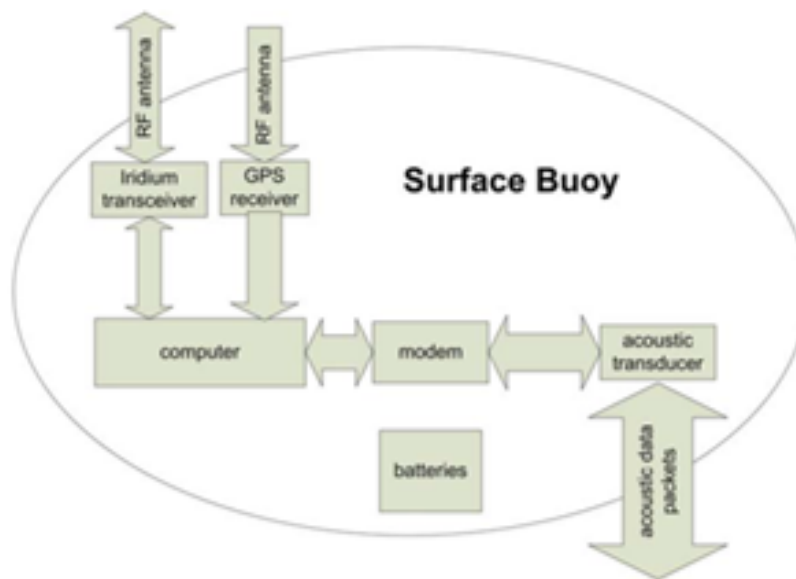


Figure 17. Components of DART II surface buoy (Meinig et al. 2005).

5.3 Cost Drivers

Potential avoided costs from marine energy integration were a main consideration in the determination of use case location. Considering operational drivers, some of the costliest DART sites were determined to be those in the Atlantic, because they are more spread out and less accessible by ship. Costs are actually even higher for the station off of Charleston because of buoy failures due to eddy currents from the Gulf Stream which are higher than those of the surrounding water; the presence of these currents may make this and similar sites attractive for

ocean current power generation. The Aleutians may also be of interest, because they are the hardest to measure; however, those stations are close together so take less ship time between stations, and were not chosen for this reason.

Capital costs for each DART II station are roughly \$200K - \$250K per site (NDBC, personal communications). Ship-based maintenance is required to replace batteries on the surface buoy and to otherwise maintain the system. The surface buoy is designed to stay out for approximately two years, but it is currently being maintained at roughly one-year intervals. For the purpose of this analysis, ship costs are assumed to be about \$20K - \$30K per day, with roughly a day needed for each station.

5.4 Energy Use

The DART II buoys have been engineered to minimize the amount of power needed for all system components (e.g., surface buoy, seafloor package, data processing, and communications) and to maximize the length of time between maintenance intervals. The total power requirement for the system is less than 1 W, with an operational max power draw of 0.1 W for the seafloor package (tsunameter computer, pressure measurement system, and acoustic modem) and 0.25 W for the surface buoy (computer, Iridium transceiver, and acoustic modem). The surface buoy's fiberglass well houses the system electronics and power supply, which is made up of packs of D-cell alkaline batteries. Alkaline batteries are designed to last for four years in the seafloor package and at least two years in the surface buoy. The computer and Iridium transceiver are powered by 2.6 kWh batteries; the acoustic modem is powered by 1.8 kWh batteries. These batteries are intended to power the buoy for at least two years.

5.5 Resource Availability

Given that surface buoys have access to a variety of resources, a combination of these may make the most sense in terms of powering the buoy (wave, solar, and wind). The current focus of this use case is on an Atlantic station off the Northeast U.S. This station, designated 44402 is located at Southeast Block Canyon, 130 NM SE of Fire Island, NY (39.287 N 70.632 W; 2,644 m depth). It was discussed as being more expensive to service due to its distance from shore and few other nearby NDBC assets. However, it is closer to other ocean observations assets (the OOI Pioneer Array) than similarly remote DART stations, and thus a more suitable candidate for further analysis including resource characterization.

DART buoys do not record ocean and meteorological data as would be required to perform a direct resource characterization at the site. Further, readily accessible models of wave and solar resources do not extend as far offshore as the selected asset, which is representative of the remoteness of DART stations. Therefore, the closest observation buoy to station 4402 is selected as a proxy for conditions. The local region and closest observation platforms are shown in Fig. A.2 in Appendix A. The OOI Coastal Pioneer array is the closest location (and location of the AUV use case), roughly 100 km distant, and is assumed representative of open ocean conditions in this part of the Atlantic. Its measurements of wind velocity, solar irradiance, and wave motion are used in this analysis. Ocean current resource is not viable due to measurements indicating speeds rarely exceed the minimum required for turbine operation. A combination of wave and solar or wind and solar are likely to yield power in great excess of the platform's current power usage throughout the year. See the Resource Availability section of Use Case #3 (4.5) for details.

5.6 Potential Partners

Potential partners who have indicated interest in this project include NDBC, who provide operation support for the buoys, and PMEL, who are in charge of the DART development lab. Key staff at each of these facilities have contributed to the development of this use case and indicated interest in the possible application of marine energy towards extending the mission of the DART buoys. As this use case moves forward, these partners will be asked to assist with identifying functional requirements and design elements for marine energy devices that will help connect marine energy power sources to the DART buoys without disrupting the essential mission of the platform.

5.7 Conclusions

Tsunami warning systems have tremendous societal and economic value by saving lives and property. Redundancy is immensely important for DART system reliability. If more power were available, the systems could be more resilient and less dependent on scheduled maintenance, other sensors could potentially be deployed (e.g., meteorological observations), and more redundancy could be added. Next steps will be to better understand NOAA's functional requirements for the system and define constraints and barriers to adapting marine energy technology for this critical infrastructure.

6.0 Use Case #5: Powering a Drifting Profiler

6.1 Introduction and Value Proposition

The ocean not only covers 71% of the planet's surface, but it also averages 2.3 miles deep. The ocean's immensity makes it challenging to measure, especially at depth. In order to measure the ocean far beneath its surface, devices must be sent to these locations. A common tool used by ocean scientists is the drifting profiler, or profiling float.

Profiling floats are programmed to sink to a pre-specified depth, or a "parking depth", and remain there for a period of time, then ascend back to the surface. The profiler can be programmed to record ocean measurements along this whole path, collecting data throughout the water column from the parking depth to the surface where it transmits data back to scientists on shore via satellite. Profilers are designed for a variety of depths and durations, some might descend to over 2,000 meters and complete over 250 cycles over their operating life.

Profilers can host a variety of sensors, measuring such things as temperature, salinity, currents, and pH, among many others. They are also relatively cheap when compared to other forms of direct ocean observations, allowing scientists to deploy thousands globally for comparatively little cost. One of the largest collections of profilers in the world is the Argo array, which as of December 15, 2019, had a total of 3,885 functional profilers deployed. This system of profilers provides invaluable data to ocean scientists all over the world which helps influence models for ocean circulation, weather, and even distribution of biomass. The value of these models to society in their ability to accurately predict weather, track fish, or numerous other services is invaluable.

The endurance of profiling floats is limited by battery capacity and sampling rate. Once the profiler float's battery can no longer power the buoyancy engine, the profiler usually ends up as flotsam or sinks to the seafloor. In order to maintain global coverage the profiler must be replaced. In the Argo program, this replacement rate amounts to about 800 profilers per year, costing an estimated \$20M (NOAA 2017).

If floats could last longer, not only would they be able to conduct more profiles and collect more data, but this would also reduce the total average cost per profile. This case study will focus on the use of marine energy to power profilers, like those used in the Argo program, to increase their operating life and the amount of data collected. From the characteristics of a typical mission for a drifting profiler there are multiple potential sources available for energy harvesting that could be utilized by profiling floats. These resources include thermal differentials, wave, current, and solar. Since drifting profilers need to operate throughout all of the world's oceans and do not remain where they are deployed, it's likely there will not be a one-size-fits-all approach and as a result, this use case did not focus on any single location.

6.2 Technology Description

A drifting profiler is an autonomous device that uses buoyancy control to maintain a specific depth. These devices spend a large portion of their life drifting in ocean currents at a specified depth below the water surface. At regular intervals the drifting profiler will descend to a programmed depth then slowly ascend to the surface. During these vertical cycles, called profiles, sensors on the profilers record environmental conditions throughout the water column. The best example of drifting profilers are Argo floats. Argo is an international array of drifting profiling floats with a core mission of collecting temperature and salinity data on a global scale. Argo is a major component of the ocean observing system and is the main of the global subsurface datasets used in all ocean assimilation models (UCSD 2019).

6.2.1 Argo Floats

Argo is a system of drifting profilers that was conceived internationally during the 1990s, with the first wide-spread deployments in 1999. A goal of Argo was to have global coverage of the world's ice-free oceans with a spacing of approximately 3° in latitude and longitude (about 300 km), for a total of around 3,000 floats, which was achieved in 2007 (Riser et al. 2016). As of December 15, 2019, there are a total of 3,885 functional Argo floats distributed throughout the world's oceans (Fig. 18a), with some now deployed in regions with seasonal ice coverage. Future plans for the Argo array, known as the Argo2020 design, include strategically doubling the density of operational floats (i.e., 2 floats per 3° square) in specific regions resulting in a target of approximately 4,600 operational Argo floats active at any time (Fig. 18b).

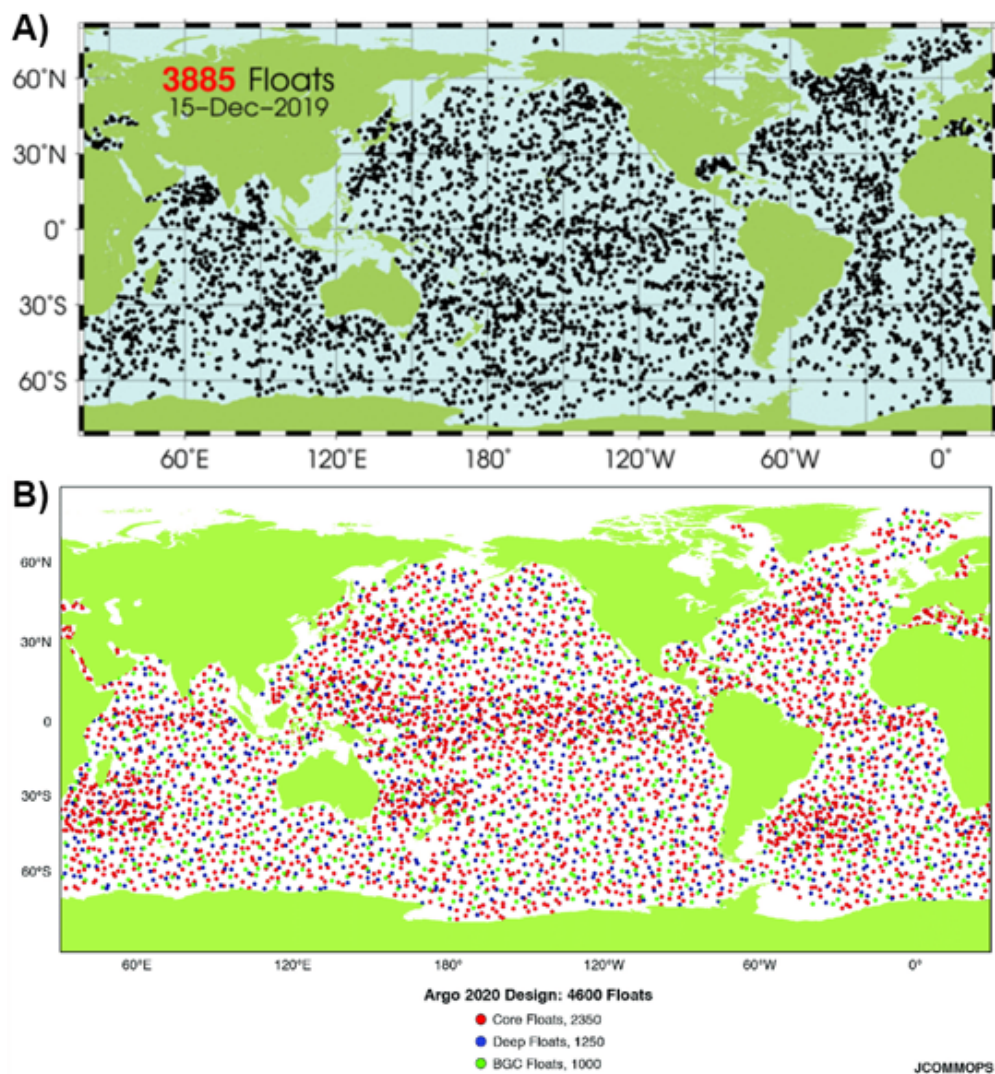


Figure 18. Map of current and planned Argo float deployment. a) Functional Argo floats, as of 12/15/2019, distributed throughout the world's oceans (Courtesy of UCSD); b) Schematic of the Argo2020 design indicating the density of the 4600 floats targeted in the system design (Source: JCOMMOPS).

Argo floats use onboard battery systems to create variable buoyancy that allow the floats to

rise and sink within the water column, taking measurements continuously on a fixed depth-derived duty cycle. Fig. 19a shows an example of one of the current models of drifting profilers currently used in the Argo array, the SOLO-II float developed by the Scripps Institution of Oceanography, a department within the UCSD. The typical size of the approved Argo floats is approximately 1.3 m long, 20 cm in diameter, and a minimum volume of 16.6 L. The weight of the Argo floats varies between the models, with the Seabird Navi having a weight of 18.5 kg, the NKE Instrumentation PROVOR I having a weight of 34 kg, and the other models falling somewhere in between.

A typical “park and profile” mission for an Argo float involves adjusting the buoyancy to maintain a “parking depth” that is typically about 1,000 m. At this depth the float will drift along with currents for approximately nine days before it conducts a profile involving the float descending down to the bottom of the profile, typically 2,000 m, and then ascending to the surface while collecting measurements on conductivity, temperature, and depth for the Core Argo floats (Fig. 19b). Once at the surface, the Argo float will use some form of satellite-based triangulation (current Argo floats rely on GPS) to estimate the current location in the ocean and will then use satellite-based communication (current Argo floats rely on the Iridium satellite constellation) to upload the location and data collected during the profile just completed. Once the data has been communicated the Argo float will descend back down to the parking depth and the cycle will repeat.

Argo floats have a typical lifespan of four to five years before the battery is depleted to a state that there is not enough power to inflate the bladder in order to bring the float to the surface, at which time it eventually sinks to the sea floor or is recovered. In order to maintain the global deployment at the current density of floats, approximately 800 new Argo floats need to be deployed each year (Roemmich et al. 2019). Assuming there are no changes to the operational lifetime, when the Argo2020 design is implemented approximately 950 Argo floats will need to be deployed each year to maintain the density of Argo floats.

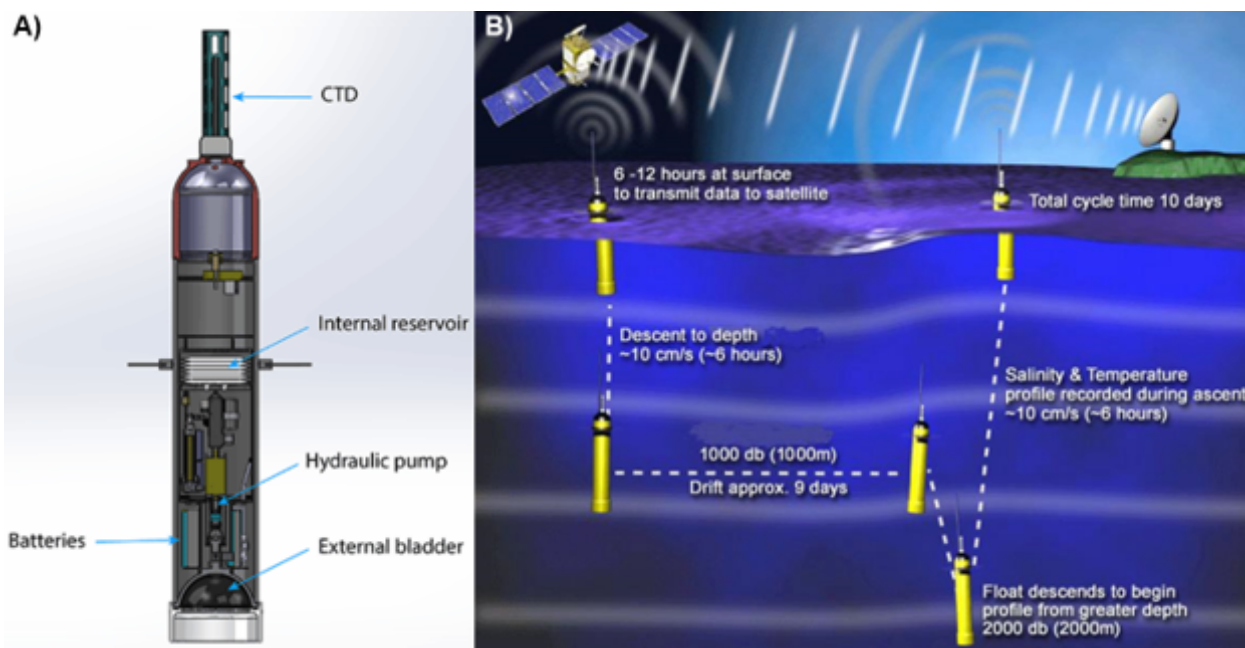


Figure 19. Example of Argo float and operation. a) Schematic of Argo SOLO-II float (Courtesy of Michael McClune at Scripps Institution of Oceanography); b) Park and profile mission operation (Courtesy of UCSD).

The Core Argo floats are the oldest most extensive system of Argo floats, collecting temperature and salinity measurements to depths of approximately 2,000 m. Although Core Argos originally were deployed in ice-free seas, they are now in use in seasonal ice zones as well. For the Argo floats deployed in the regions above 60° latitude, during the period of ice cover the float will continue to operate but with the profiles not reaching the water surface where ice would be encountered. Once the ice melts the float will switch to normal operation, and once on the surface all of the profile data collected over the ice-covered period will be uploaded. Some of these floats use a system known as RAFOS that involves including an acoustic receiver in the float and deploying an array of fixed acoustic transmitters with a range of approximately 500 km in order to perform geolocation when the float is unable to reach the surface to utilize the GPS.

Biogeochemical (BGC) Argos also include sensors that collect measurements associated with uptake of carbon in the oceans, ocean acidification, and decreases of dissolved oxygen in ocean water (i.e., pH, oxygen, nitrate, chlorophyll, suspended particles, and downwelling irradiance). Deep Argos are designed to take physical measurements to depths of 6,000 m and have only been deployed under pilot projects to date (Roemmich et al. 2019).

Each Argo float is also equipped with communications gear for remote data uplink to the Argo Data Assembly Centres (DACs). Argo floats utilize GPS for location and the Iridium satellite constellation for data uplink. The advantage of using the Iridium satellite constellation is that the data transmission rate and the number of satellites in the constellation allows for much faster data uplink. While Argo floats using an older communications network could require staying at the surface for up to 12 hours, floats using Iridium now require only 20 minutes, which saves energy, reduces biofouling, and reduces risks of drifting into shallow water (Roemmich et al. 2009). In addition, the communication provided by Iridium constellation is two-way, allowing for commands to be sent to individual Argo floats to set parameters such as parking depth, profile starting depth, depth resolution for the profile, or any other useful operational parameters.

6.3 Cost Drivers

Costs for the equipment, deployment, data handling, and program management are based off of reporting from UCSD and NOAA. The cost of a single Argo float can be up to \$20K, however when the costs of deploying the float, handling the data collected, and running the program are considered the total per float cost can increase up to double of the device cost (UCSD 2019). The typical expected minimum lifetime of an Argo float is around four years. In order to maintain the current density of the array, around 800 new floats must be deployed (Roemmich et al. 2009) at a total annual maintenance cost of about \$20M (NOAA 2017). This results in a typical cost of about \$200 per profile collected. Considering the increased number of floats in the Argo2020 design, assuming no other changes, the total annual maintenance cost would increase accordingly.

Another significant upcoming cost for the Argo program will come when the pilot program for the BGC Argo moves to full global implementation. It is estimated that in order to understand biogeochemical processes on a global scale a total of 1,000 BGC profiling floats will be needed. Depending on the model of the BGC float, the cost can range from \$25K to \$120K (Xing et al. 2018), but the average lifetime cost for a BGC float when all things are considered is approximately \$100K. Given the similar lifetime for the BGC floats of four years, maintenance for the BGC array will require deployment of 250 BGC floats per year at an estimated annual cost of \$25M (Roemmich et al. 2009).

One of the most significant cost drivers is deployment costs. More specifically, the

deployment costs can include vessel costs that can be on the order of \$20-\$25K per day. If the lifetime of the float could be increased through energy savings, energy harvesting from the environment, or strategies to efficiently service the floats prior to battery depletion, then the average cost per profile can be reduced by lowering the number of new devices that must be purchased and deployed each year.

Not only does increasing the longevity of the floats reduce the annual replacement costs, but it could also reduce the hidden costs related to ocean waste. A recent review paper on the global ecological, social, and economic impacts of marine plastic conducted a literature review of 1191 data points to estimate that the economic cost of marine plastic is between \$3.3K to \$33K per metric ton per year (Beaumont et al. 2019). This range covers only marine natural capital impacts, and therefore the full economic cost is likely significantly higher. Given the number of floats deployed per year that will not be recovered and the long-term ongoing nature of the program, increasing the lifetime of the floats can have additional benefits that might not be readily apparent.

6.4 Energy Use

Most of the energy used by an Argo float is consumed during the profiling portion of the mission where the pump is used to change the buoyancy, the sensors are sampled while ascending the water column, and the satellite communication is used for data-uplink. A report published in 2017 that investigated how lithium batteries work and behave in Argo floats (Gordon 2017) documented that the range of energy use per profile for the different models of Core Argo floats was in the range of 2.8 Wh to 4.4 Wh. For the Core Argo floats, the total battery energy is about 1.1 kWh to 1.4 kWh.

The energy to power the float is primarily provided by one of two options for the primary (i.e., non-rechargeable) lithium batteries, Electrochem's CSC93DD cells and Tadiran's TL6930 cells. The report documents that the battery efficiency (i.e., percentage of battery energy used for float operation) ranges between 50 to 75%. Given these battery constraints, at a 10-day profile interval current models of Core Argo floats can achieve about 200 to 250 profiles before the battery is too depleted to return to the surface.

BGC Argo floats, which are currently in the global pilot scale stage of deployment, are similar to Core Argo floats with the inclusion of additional biogeochemical sensors. As a result of the additional sensors, the percentage of the total battery energy that is consumed by the sensors is about 25%. An example of the energy breakdown averaged over 374 profiles for an Apex float with nitrate and oxygen sensors, in addition to the standard conductivity and temperature sensors, is given in Table 4.

To investigate the energy use of Deep Argos, which are also currently in the global pilot scale stage of deployment, one can look at the MRV Deep SOLO (Roemmich et al. 2019). The Deep SOLO includes five hybrid battery packs containing about 1.9 kWh of useful energy. Given the much deeper starting depth for the profiling, the per profile energy expenditure is about 7.5 Wh or about double that of the Core Argo floats. This results in a float that can achieve between 200 to 250 profiles providing an estimated lifetime between five to seven years, although these lifetimes have not yet been confirmed.

If it were possible to increase the energy available to the profiler through means such as design changes that reduce power draw (e.g., the switch to the Iridium satellite constellation), energy converters that harness energy from the environment to supplement the energy contained within batteries at deployment, or through design changes that allow the profilers to be serviced in an economically viable way, than the next logical question would be how to best use the additional energy available.

Table 4. Energy breakdown by components for a Teledyne Apex float with nitrate and oxygen sensors averaged over 374 profiles (Gordon 2017).

Component	Percentage of Energy (%)	Mean Energy per Profile (Wh)
Buoyancy engine	28.9	1.1
Primary controller	10.0	0.4
Localization and telemetry	13.9	0.5
Nitrate sensor	21.3	0.8
Oxygen sensor	0.6	0.03
CTD sensor	20.2	0.8
Battery self-discharge	5.0	0.2
Total	100	3.83

The most readily available option would be to simply increase the total number of profiles at either the same rate, extending the lifetime, or at an increased rate. Another option would be to increase the vertical resolution of the data collected during the profile. For example, in Table 4 if the power used by the nitrate sensor is ignored, as it is not a part of the Core Argo floats, the second largest use of power is from the CTD sensor and the third largest power draw is from the use of the Iridium satellite modem for communication. The CTD for this float collects 500 CTD samples during a profile and uses 0.002 Wh per CTD measurement, for a total of 0.8 Wh per profile. If the vertical resolution were doubled the total mean energy per profile would increase by over 25%, especially when the increased energy required to transmit the additional data is also taken into account.

A more sophisticated use of the increased energy availability could be for implementing systems that would allow the drifting profiler to alter its trajectory through either passive or active means. It is known that Argo floats can get caught in ocean gyres, so it would be advantageous if there were a way to autonomously free the float from the gyre. Altering the floats trajectory could be done passively through the use of articulated fins, potentially using a type of fins known as grid fins which are flight control surfaces used by SpaceX (along with other rockets or missiles) to passively steer their reusable launch system to the landing site as it falls back to earth at high velocities (SPACEX 2015).

Another possible use could be guiding a float that is nearing the end of its expected lifetime toward land or a research vessel where it could be readily recovered, batteries replaced, sensors calibrated, and then redeployed. It is also possible that the ability to alter a float's trajectory could be utilized to steer a float toward a theoretical recharging station. While passive means to alter the trajectory may be able to guide the float to a general location, moving the float to within a short enough range to use inductive charging to transfer power would likely require active means. A single thruster could be incorporated into the float that could be used in conjunction with the fins. To avoid complications that could arise from propelling the float near the surface, the thrust and steering could be applied while the float is submerged at the parking depth. This could require underwater geolocation to provide a target for the float to move toward. As mentioned in a previous section, some Argo floats that operate in polar regions under ice are currently configured to use the RAFOS system for underwater geolocation.

RAFOS transmitters could be deployed around a recharging station in order to provide a means for a float to move towards a target while submerged without resurfacing to acquire a GPS fix. These RAFOS transmitters could also be powered by whatever marine energy converter technology is used to provide power to the recharging station.

Another potential use for the increased energy could be used for dealing with biofouling of the sensors. Currently given the characteristics of the Argo missions (i.e., primarily submerged at 1000 m for extended periods of time) biofouling is not an issue. However other forms of drifting profilers could need to operate in shallower sunlit waters where biofouling could be a concern. In a scenario like this, power could be used to handle the biofouling through means such as exposing elements to UV light or mechanical wipers.

6.5 Resource Availability

The characteristics of the missions executed by drifting profilers largely dictates what resources could be feasible to extract energy from. During the nine day period when the profiler is drifting at the typical 1000 m parking depth, there are few resources available due to low levels of: solar radiation reaching this depth, changes in temperature during the drift, velocity differential between the profiler and surrounding water, and surface wave influence. As a result, the portions of the missions that have the best potential for extracting energy from the environment are during the profiling and when the profiler is floating at the surface.

When the profiler is ascending through the water column it is moving from cold high-pressure water to the surface where there is warmer water at atmospheric pressure. In addition, during the profiling the buoyancy engine is generating vertical motion from changes in buoyancy which provides an opportunity to harvest energy from the water current induced by the vertical forcing. When the profiler reaches the surface a small portion of the device will extend out of the water allowing for the potential to extract energy from solar radiation (discussed in more detail below), and at the surface the device is within the influence of surface waves creating the potential to extract energy from the waves.

6.5.1 Thermal Power

Ocean thermal energy is formed by the temperature difference between water at the sea surface and water in the deep sea. In tropical or semitropical areas, the temperature of surface seawater can be as high as 29°C, while below 1000 m depths the temperature can be as low as 4°C. Compared to other forms of ocean energy, ocean thermal energy is reliably and predictably available at all hours, it can be harvested while untethered, and it exploits a reasonably simple engine design. Nevertheless, thermal energy harvesting has its obvious limitations; the most important is that the extent of the temperature gradient is not globally uniform.

Since late 1990s, ocean thermal energy has been utilized by several groups throughout the world to power underwater vehicles such as profiling floats and underwater gliders, predominantly using phase change material (PCM). Because the profiler moves vertically and through the thermocline, the solid-liquid PCM can be used as a working fluid to convert thermal energy to mechanical or electrical energy reliably and predictably (Fig. 20). During the melting process, the PCM absorbs large amounts of latent heat. During the solidification process, stored thermal energy is released. The phase transition of PCMs is a transient and non-linear heat transfer phenomenon.

- Webb Research Corporation demonstrated an underwater glider propelled by environmental energy during the late 1990s and early 2000s (Webb, Simonetti, and Jones 2001). The

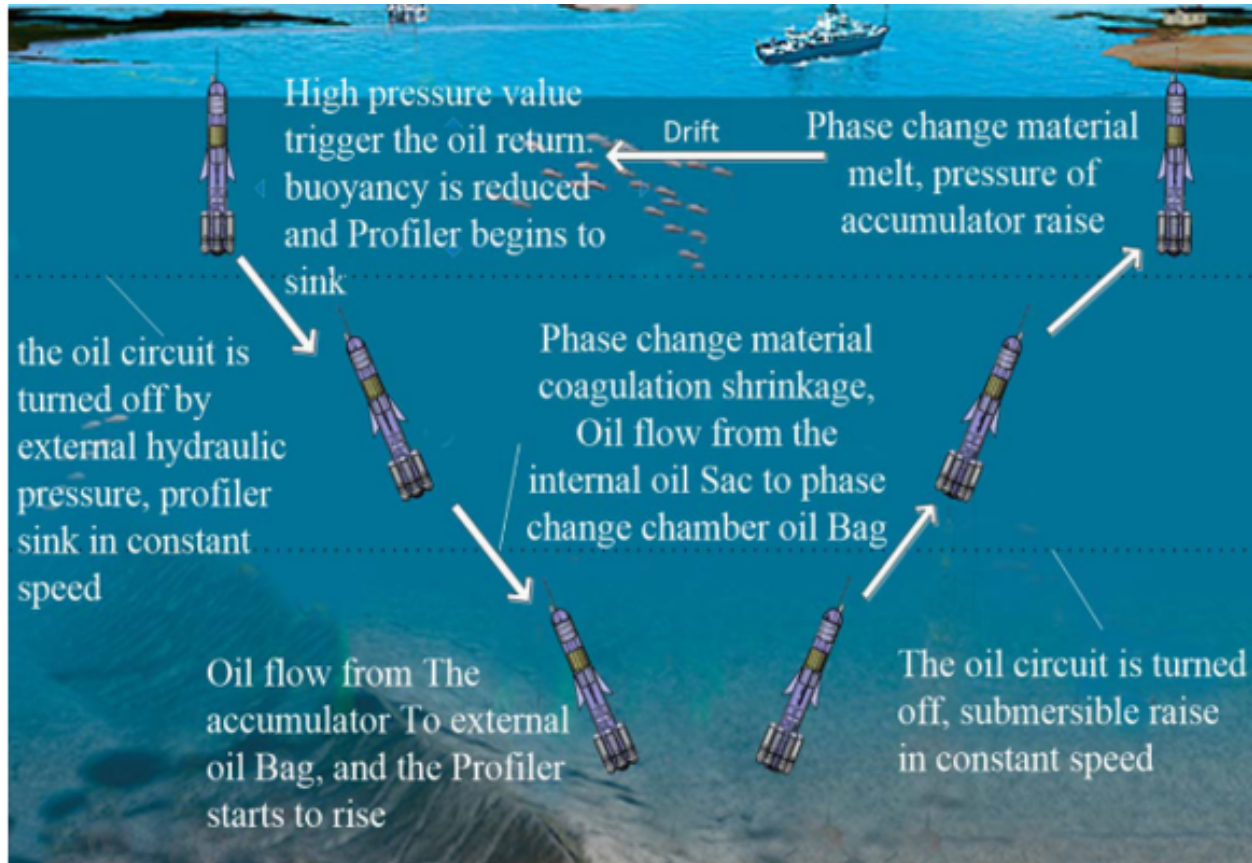


Figure 20. Schematic diagram of profiler motion in the sea (Xia et al. 2017).

engine propels the glider by changing the vehicle buoyancy. Heat is absorbed from the warm surface water and rejected to the cooler, deep water during the vehicle’s transit through the thermocline, which causes a change of state of an internal working fluid which, as a result of the phase change, undergoes a change in volume. The resulting volume change of the fluid provides an adequate change in buoyancy to the vehicle of constant mass to enable it to ascend and descend at a useful speed. This variable buoyancy, derived from environmental energy, is the sole source of the glider’s propulsion power.

- Researchers from Tianjing University, China developed a prototype of a thermal underwater glider and tested it in the South China Sea (Ma et al. 2016). It worked continuously for 29 days without any failure. The total number of working profiles collected was 121, the total cruising range was 677 km, the maximum system pressure was 12.5 MPa, the total energy harvested was 83 Wh, and the average stored energy of each cycle was 0.7 Wh. The energy stored during each profile can be derived through a nonlinear model,

$$E = -P_0V_0 \ln\left[1 - \frac{m}{V_0} \left(\frac{1}{\rho_l} - \frac{1}{\rho_s}\right)\right], \tag{1}$$

where P_0 , V_0 , m , ρ_l , and ρ_s are the initial pressure of nitrogen, initial volume of nitrogen, mass of nitrogen, liquid phase density, and solid phase density of nitrogen (Ma et al. 2016). The average theoretical value of stored energy per cycle is 1.6 Wh, whereas the actual value of stored energy is 0.7 Wh. This reduction is caused by the compressibility of the PCM and air in the system.

- Seatrec developed a prototype thermal recharging underwater float (TREC) (Chao 2016). It went beyond the buoyancy engine developed by Webb, Simonetti, and Jones 2001 by converting the ocean thermal energy to electricity for battery recharging (Chao 2016). This design reduces the risk resulting from one or more failures of the thermal energy conversion cycle. It was integrated with an existing float known as the Sounding Oceanographic Lagrangian Observer (SOLO), which is one of the approved Core Argo floats. The SOLO-TREC was deployed in 2009 southwest of the Hawaii Islands. It was programmed to dive every 8 hours between the surface and 500 meters to collect vertical profiles of temperature and salinity. By June 2011, SOLO-TREC has made more than 1000 dives between the surface and a depth of 500 meters, generating 1.4 kWh of power. Seatrec currently offers their first product, the SL1 Profiling Float Thermal Engine (length: 153.7 cm, diameter: 17.3 cm, weight in air: 30.2 kg), which supplies 2.2 Wh per cycle and is available for integration with profiling floats including the Argo variant of the Sea-Bird Scientific Navis Profiling Float.
- Researchers from Universiti Tunku Abdul Rahman, Malaysia explored an energy harvesting technique based on a thermoelectric generator (TEG) for powering floating wireless sensor nodes (Lee et al. 2018). In their design, the temperature gradient between the two TEG surfaces was achieved by attaching a heat sink to the cold side of TEG, which is in contact with the water flow for maximizing heat dissipation, and a heat source attached to the hot side of TEG, which is exposed directly to sunlight. In the actual implementation, an array of seven TEGs were connected in series to increase the available voltage from the small temperature differences, which is capable of harnessing 0.4 Wh of power during a sunny day (with a peak temperature difference of 6°C). This design is limited by the thermal gradient available between both sides of the TEG and by the number of TEGs connected in series due to the spatial requirement of heat sinks.

6.5.2 Wave Power

A wide variety of wave energy converters were proposed to extract power from the ocean. These designs differ in their structural configuration, as well as in the energy conversion technology they use. However, there are engineering challenges associated with integrating wave energy converter technologies into a profiling float. This section outlines an effort targeted explicitly on powering an underwater profiling float.

Scripps Institution of Oceanography developed an autonomous wave-powered vertical profiler, called Wirewalker (WW) (Rainville and Pinkel 2001). The profiler moves vertically along a wire which is suspended between a surface float and a weight at a depth of tens or hundreds of meters (Fig. 21a). This system derives the power needed to move vertically in the water from the energy of surface waves, and the horizontal movement of the system follows the ocean currents. A one-way clamp provides the mechanism by which wave action acting on a surface float sends a buoyant instrument package down a mooring line (Fig. 21b). In moderate sea states, the WW profile descends at a speed of 10-20 m/min and ascends at a speed of 0.5 m/s, as set by its buoyancy and drag. The principal weakness of the system lies in its mechanical wear at the top of the cycle where the cam is reengaged. This impact repeatedly occurs at an identical spot on the wire. Using a 3/16-inch galvanized wire for typical deployments, the researchers found that the wire began to fail after 10,000 profiles.

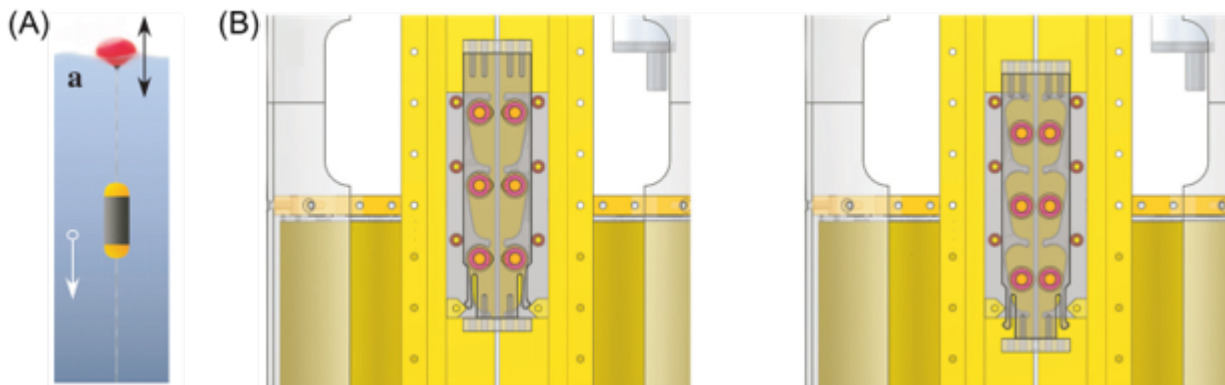


Figure 21. a) A schematic of the Wirewalker vertical profiler. Vertical motion of the surface float is transferred to the weighted deployment wire and rectified by a cam in the profiler. b) Schematic of the Wirewalker cam during ascent and descent. (Pinkel et al. 2011)

6.5.3 Current Power

The buoyancy engine used to generate vertical motion, to perform the profiling, effectively generates water current by forcing the profiler vertically through water with little natural vertical motion. This induced water current creates an opportunity to incorporate a current energy converter into a drifting profiler. This section outlines an effort to incorporate a current energy converter into a drifting profiler, as well as describes a commercial device that exploits this vertical motion to generate rotational motion that is used in a method to measure depth dependent water currents during the profiling.

- Researchers from Shandong University, China proposed a marine current energy converter for deep-water profiling floats (Fig. 22). The design incorporates a two-way energy harvesting turbine to capture the energy from the horizontal movement of the current and vertical movement of the float which converts the kinetic energy into electrical energy. In the shallow sea where ocean current energy density is high, the horizontal current energy dominates the energy generation, whereas in the relatively calm deep sea, the relative flow energy caused by the floats' autonomous up and down is the main contributor to energy generation. This captured energy is then utilized to charge the battery and extend the working hours of the floats. Further analytical and simulation results of the proposed system are available in (Wu, Liu, and An 2018). Nevertheless, this design has not been experimentally validated, and the level of power output is expected to be orders of magnitude lower than a traditional marine current conversion system.

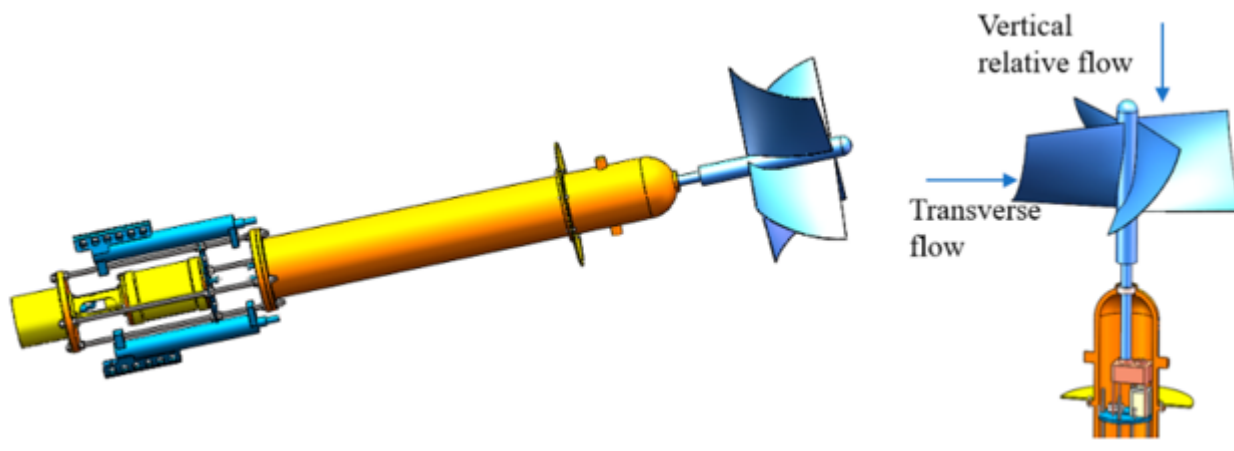


Figure 22. 3D drawing of profiling float with a characteristic diameter less than 0.4 meter and schematic diagram of the internal profile of the turbine connecting mechanism. (Wu, Liu, and An 2018)

- Teledyne Marine, vendors for the APEX line of Argo floats which compose 60% of the Argo fleet, produce a version of their float that is capable of directly measuring depth dependent water current during the profiling (Fig. 23). This float induces a rotational motion to itself using a vane ring consisting of 16 blades around the body which generates rotation while the float is being forced through the water column (Sanford et al. 2005). The vane ring diameter was constrained in size by the constraints imposed by an air deployment package. During the profiling the vane ring causes the float to rotate at a period of 12 s (Sanford, Price, and Girtton 2011). This rotational motion is used in a method for precisely measuring the water current using motionally-induced electric fields.



Figure 23. Photo of the Teledyne Marine APEX Current Profiling Float which utilizes a vane ring to generate rotational motion during a profile, which is involved in a process of directly measuring water current using motionally-induced electric fields.

6.5.4 Solar Power

To the best of our knowledge, drifting profilers like those composing the Argo array have not attempted to integrate solar energy harvesting. Traditional solar panels composed of silicon are heavy and can weigh 10 to 20 kg/m² (Addin 2011), and as a result could compromise the performance of the buoyancy engine of the profiler. Thin-film solar cells weigh as little as 1.9 kg/m² (Wang et al. 2015), and thus may be a feasible component to add to drifting profilers to harvest power without adding significant weight. There are four common material compositions used to make thin-film photovoltaic (PV) cells (Ullal 2008):

- Amorphous Silicon (a-Si): a-Si solar cells were developed in 1976 with initial 2.7% conversion efficiency. Current conversion efficiency of a-Si is stabilized at 12% to 13%.
- Cadmium Telluride (CdTe): CdTe solar cell is a promising PV technology. Theoretical efficiency for CdTe solar cell is about 26%. Laboratory efficiency of 16.5% for thin-film CdTe has been demonstrated.
- Copper Indium Gallium Selenide (CIGS): CIGS has demonstrated the highest conversion efficiency among any thin-film solar cells in the range of 19.3% to 19.9%.

If photovoltaic cells were to be incorporated into a drifting profiler, it is likely that it would be using one of the thin-film PV cells listed and not the more common silicon PV cells. As mentioned in a previous section, a typical Core Argo float is about 1.3 m long and about 20 cm in diameter. The design of the floats includes a stability disk (Fig. 24a) that is intended to stabilize the float while at the surface to improve the performance of the satellite communication. If it is assumed that a thin-film PV cell can be attached to the entire surface on and above the stability disk it is possible to estimate the area.

From available literature it is unclear what the distance is from the top of the main cylindrical body of the float to the stability disk is and also what the diameter of the stability disk is. From photos of the various approved Argo floats it would appear that the distance varies between approximately 10 to 50 cm from the top. In addition, the diameter of the stability disk appears to be on the order of two to three times the diameter of the float itself (Fig. 24b). For the analysis it is assumed that the diameter of the stability disk is 60 cm, resulting in an area of 0.25 m², the top of the float is completely obscured (e.g., sensors, GPS, Iridium antenna), and the vertical distance to the stability disk is in a range between 0.01 to 0.05 m, resulting in an area of $0.628 * L$ m² where L is the vertical distance. It will be assumed the power generation of the thin-film PV cell is 180 W/m² (Banpil Photonics 2019).

The amount of time at the surface, the latitude, and the time of day when the float is at the surface is variable, so for the analysis it will be assumed that the float is at the surface for six hours at peak light intensity. It is assumed that the power generated will be stored in rechargeable batteries with a charging efficiency of 90%. Given the cylindrical shape, depending on the latitude and time of day it is likely the effective area of the PV cell receiving full illumination is considerably less than the full area, so for this analysis it is assumed that only one quarter of the PV cell is exposed to full illumination. This results in the estimated power of:

$$P = 180 \frac{A}{4}, \quad (2)$$

where P is the power in W and A is the full area of the PV cell. Assuming a range of distances to the stability disk, power output may range from 14-25 W and 76-137 Wh of energy may be stored from six hours in full sun.

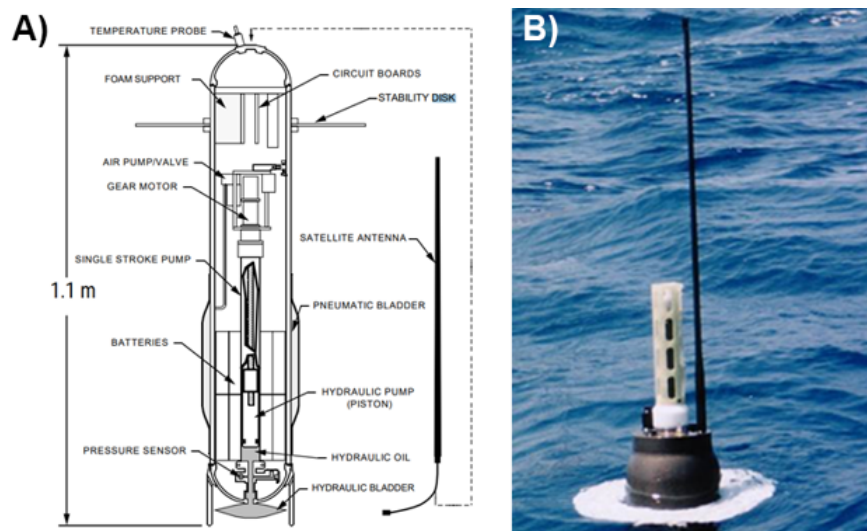


Figure 24. General size and location of the stability disk of an Argo float. a) Schematic of a SOLO float (Bishop et al. 2003); b) Photo of a PROVO float at the water surface

6.6 Potential Partners

The most important potential partner is the Argo Steering Team (AST), which provides scientific leadership and oversees the development and implementation for the Argo array of profiling floats. Other potential partners can be broken down into several categories for which there are several potential partners for each category: research organizations which have been instrumental in the development of the Argo program, governmental agencies and labs involved in the Argo program, commercial vendors of Argo profiling floats and/or the sensors approved for Argo profiling floats, and battery vendors. A breakdown of the potential vendors is listed below:

- **Argo Steering Team**
- **Research Organizations:**
 - Scripps Institution of Oceanography, UCSD
 - University of Washington
 - WHOI
- **Government agencies and labs:**
 - NOAA's Atlantic Oceanographic and Meteorological Laboratory (AOML)
 - PMEL
 - CSIRO Oceans and Atmosphere
- **Argo and instrument vendors:**
 - MRV Systems: vendor for Argo floats such as DEEPSOLO and SOLO-II
 - Seabird: vendor for CTD sensor and Argo floats such as Navis Float
 - Teledyne Marine: vendor for Argo floats such as APEX Argo and APEX BioGeoChem
 - NKE Instrumentation: vendor for Argo floats in UK
 - The Tsurumi Seiki Co: vendor for Argo floats in Japan

- RBR Global: vendor for Argo components such as CTD in Canada (AST has approved RBR for a “Global Pilot” deployment)
- **Battery vendors:**
 - Seatrec Inc: a startup developing rechargeable battery recharged using thermal energy
 - Tadiran Batteries: existing vendor for the primary lithium batteries
 - Electrochem: existing vendor for the primary lithium batteries

6.7 Conclusions

Drifting profilers, such as the ones composing the Argo array, are an important component of the ocean observing system. The Argo program is a large ongoing international program with significant maintenance costs largely related to deploying enough drifting profilers to maintain the density of the array. As the Argo program continues, the ongoing costs will continue to increase as new objectives move from the pilot stage into the full global implementation phase, such as the upcoming change to move the BGC Argo pilot into full global implementation.

If energy could be harnessed from the environment to supplement the power available to the drifting profiler, the lifetime of a given profiler could be extended, reducing operation costs, increasing the sampling rate during profiles, and/or new capabilities could be added to extend the versatility of this type of device. From the characteristics of a typical mission for a drifting profiler there are multiple potential sources of energy that could be extracted during the profiling portion of a mission. These include thermal, wave, current, and solar. Since drifting profilers need to operate globally there may not be a one-size-fits-all approach to harvesting energy. As a result, this use case did not focus on a single location.

7.0 Conclusion

The identification, description, and exploration of the use cases demonstrates that there is significant potential for marine energy to provide power for a range of ocean observation platforms, sensors, and missions. The five use cases cover a range of fixed and mobile platforms that are representative of present and anticipated future ocean observation missions. The platforms represented by each use case could be adapted for receiving alternate or additional forms of renewable energy to: extend range; increase sampling rate; add and operate additional sensors; reduce observation mission costs and risks; and/or to increase the stealth of subsurface surveillance missions.

Each use case has been examined through the lens of practicality, cost, and availability of renewable energy sources at the selected sites. For most of the use cases, a mix of existing or new renewable energy sources, most notably solar power, combined with adequate power storage, would enable marine energy technologies to support present and future missions. For the selected locations, wave or tidal current power is the strongest available resource.

The next step in the use case investigation will examine functional requirements, subject to constraints and barriers, to adapting marine energy system designs to meet the needs uncovered in the descriptions of the five use cases. This would be followed by development of design requirements for the marine energy devices that could power them. As an output of the process, future research and development needs will be identified to enable building and testing of marine energy devices that will realize the promise of powering of ocean observations with marine renewable energy.

Acknowledgements

AE Copping, RJ Cavagnaro, JJ Martinez, and Y Yang are with the Pacific Northwest National Laboratory. RE Green, DS Jenne, and DM Greene are with the National Renewable Energy Laboratory. Thanks to the members of the ocean observing community, whose feedback and engagement were crucial to this work, including individuals from NOAA, UAF, APL-UW, UCSD, WHOI, MBARI, and manufacturers and vendors of some of the platforms discussed within.

References

- Addin, Burhan K Saif. 2011. “The Challenges of Organic Polymer Solar Cells.” Master’s thesis, Massachusetts Institute of Technology.
- Babarit, Aurélien. 2015. “A Database of Capture Width Ratio of Wave Energy Converters.” *Renewable Energy* 80:610–628.
- Banpil Photonics. 2019. “Banpil Photonics, Inc. - Photovoltaic Solar Cells.” (Accessed on 12/30/2019).
- Beaumont, Nicola, Margrethe Aanesen, Melanie Austen, Tobias Börger, James Clark, Matthew Cole, Tara Hooper, Penelope Lindeque, Christine Pascoe, and Kayleigh Wyles. 2019. “Global Ecological, Social and Economic Impacts of Marine Plastic.” *Marine Pollution Bulletin* 142:189–195.
- Bernard, Eddie, and Christian Meinig. 2011. “History and Future of Deep-Ocean Tsunami Measurements.” In *OCEANS’11 MTS/IEEE KONA*, 1–7. IEEE.
- Bishop, James, Christopher Guay, Jeffery Sherman, Casey Moore, and Russ Davis. 2003. “Prospects for a “C-ARGO”: A New Approach for Exploring Ocean Carbon System Variability.” In *Proceedings of the International Workshop on Autonomous Measurements of Biogeochemical Parameters in the Ocean. Honolulu, HI, CDROM*.
- Blue Logic. 2019. *Subsea Docking Station (SDS)*. <https://www.bluelogic.no/news-and-media/subsea-docking-station-sds->. (Accessed on 12/27/2019).
- Cahill, Brendan, and Tony Lewis. 2014. “Wave Period Ratios and the Calculation of Wave Power.” *The 2nd Marine Energy Technology Symposium*, 1–10.
- Chao, Yi. 2016. “Autonomous Underwater Vehicles and Sensors Powered by Ocean Thermal Energy.” In *OCEANS 2016 - Shanghai*, 1–4. IEEE.
- CODAR. 2019a. *General Specifications*. http://www.codar.com/SeaSonde_gen_specs.shtml. (Accessed on 12/27/2019).
- . 2019b. *The SeaSonde*. http://www.codar.com/images/products/SeaSonde/1A-SeaSonde_v2_20100331.pdf. (Accessed on 12/27/2019).
- Dobos, Aron. 2014. *PVWatts Version 5 Manual*. Technical report. National Renewable Energy Lab.(NREL), Golden, CO (United States).
- Fan, Shuangshuang, Chenzhan Liu, Bo Li, Yuanxin Xu, and Wen Xu. 2019. “AUV Docking Based on USBL Navigation and Vision Guidance.” *Journal of Marine Science and Technology* 24 (3): 673–685. ISSN: 1437-8213. <https://doi.org/10.1007/s00773-018-0577-8>. <https://doi.org/10.1007/s00773-018-0577-8>.
- Gilman, Paul. 2015. *SAM Photovoltaic Model Technical Reference*. Technical report. National Renewable Energy Lab (NREL), Golden, CO (United States).
- Gordon, Lee. 2017. *Recommendations for Reports About Argo Float Batteries*. Technical report. University of California San Diego (UCSD).

- Green, Rebecca, Andrea Copping, Robert Cavagnaro, Deborah Rose, Dorian Overhus, and Dale Jenne. 2019. *Enabling Power at Sea: Opportunities for Expanded Ocean Observations through Marine Renewable Energy Integration Preprint*. Technical report. National Renewable Energy Lab.(NREL), Golden, CO (United States).
- Kohler, Craig, Lex LeBlanc, and James Elliott. 2015. "SCOOP-NDBC's New Ocean Observing System." In *OCEANS 2015-MTS/IEEE Washington*, 1–5. IEEE.
- Kongsberg. 2019. *Autonomous Underwater Vehicle, REMUS 600 - Kongsberg Maritime*. <https://www.kongsberg.com/maritime/products/marine-robotics/autonomous-underwater-vehicles/AUV-remus-600/#technicalInformation>. (Accessed on 12/30/2019).
- Lee, Wai-Kong, Martin Schubert, Boon-Yaik Ooi, and Stanley Jian-Qin Ho. 2018. "Multi-Source Energy Harvesting and Storage for Floating Wireless Sensor Network Nodes with Long Range Communication Capability." *IEEE Transactions on Industry Applications* 54 (3): 2606–2615.
- Lenee-Bluhm, Pukha, Robert Paasch, and H. Tuba Özkan-Haller. 2011. "Characterizing the Wave Energy Resource of the US Pacific Northwest." *Renewable Energy* 36 (8): 2106–2119.
- Ma, Zhesong, Yanhui Wang, Shuxin Wang, and Yanan Yang. 2016. "Ocean Thermal Energy Harvesting with Phase Change Material for Underwater Glider." *Applied Energy* 178:557–566.
- Maslin, Elaine. 2019. *Seaspace Race Underway at Saab Subsea Docking*. <https://www.oedigital.com/news/467483-seaspace-race-underway-at-saab-subsea-docking-demo>. (Accessed on 12/30/2019).
- MBARI. 2019. *Autonomous Underwater Vehicle Docking*. <https://www.mbari.org/autonomous-underwater-vehicle-docking/>. (Accessed on 12/30/2019).
- Meinig, Christian, Scott Stalin, Alex Nakamura, and Hugh Milburn. 2005. "Real-Time Deep-Ocean Tsunami Measuring, Monitoring, and Reporting System: The NOAA DART II Description and Disclosure." *NOAA, Pacific Marine Environmental Laboratory (PMEL)*, 1–15.
- NDBC. 2018. *Programmatic Environmental Assessment for the National Oceanic and Atmospheric Administration National Data Buoy Center*. Technical report. NOAA NDBC, Stennis Space Center, MS (United States).
- . 2019a. *NDBC DART® Program*. <https://www.ndbc.noaa.gov/dart.shtml>. (Accessed on 12/31/2019).
- . 2019b. *Station 46077 Recent Data*. https://www.ndbc.noaa.gov/station_page.php?station=46077. (Accessed on 12/27/2019).
- . 2019c. *Station DRFA2 Recent Data*. https://www.ndbc.noaa.gov/station_page.php?station=drfa2. (Accessed on 12/27/2019).
- NOAA. 2017. *NOAA 200th Feature Story: Argo Floats*. <https://celebrating200years.noaa.gov/magazine/argo/welcome.html>. (Accessed on 12/30/2019).
- NREL. 2019. *MHK Atlas*. <https://maps.nrel.gov/mhk-atlas/>. (Accessed on 12/31/2019).

- O'Donnell, James, and Neal Pettigrew. 2008. *NERACOOS HF RADAR Gap Analysis*. Technical report. Northeastern Regional Coastal Observing System, Portsmouth, NH (United States).
- OOI. 2019. *CP01CNSM | Ocean Observatories Initiative*. <https://oceanobservatories.org/site/cp01cnsm/>. (Accessed on 12/30/2019).
- Pinkel, Robert, Michael Goldin, Jerome Smith, Oliver Sun, Anthony Aja, Mai Bui, and Tyler Hughen. 2011. "The Wirewalker: A Vertically Profiling Instrument Carrier Powered by Ocean Waves." *Journal of Atmospheric and Oceanic Technology* 28 (3): 426–435.
- Rainville, Luc, and Robert Pinkel. 2001. "Wirewalker: An Autonomous Wave-Powered Vertical Profiler." *Journal of Atmospheric and Oceanic Technology* 18 (6): 1048–1051.
- Riemer, Tara. 2015. *Proposal for FY2016-2020 Implementation and Development of Regional Coastal Ocean Observing System: Alaska Ocean Observing System*. Technical report. Alaska Ocean Observing System, Anchorage, AK (United States).
- Riser, Stephen, Howard Freeland, Dean Roemmich, Susan Wijffels, Ariel Troisi, Mathieu Belbéoch, Denis Gilbert, Jianping Xu, Sylvie Pouliquen, and Ann Thresher. 2016. "Fifteen Years of Ocean Observations with the Global Argo Array." *Nature Climate Change* 6 (2): 145–153.
- Roemmich, Dean, Matthew Alford, Hervé Claustre, Kenneth Johnson, Brian King, James Moum, Peter Oke, W. Brechner Owens, Sylvie Pouliquen, and Sarah Purkey. 2019. "On the Future of Argo: A Global, Full-Depth, Multi-Disciplinary Array." *Frontiers in Marine Science* 6.
- Roemmich, Dean, Gregory Johnson, Stephen Riser, Russ Davis, John Gilson, W. Brechner Owens, Silvia Garzoli, Claudia Schmid, and Mark Ignaszewski. 2009. "The Argo Program: Observing the Global Ocean with Profiling Floats." *Oceanography* 22 (2): 34–43.
- Sanford, Thomas, John Dunlap, James Carlson, Douglas Webb, and James Girton. 2005. "Autonomous Velocity and Density Profiler: EM-APEX." In *Proceedings of the IEEE/OES Eighth Working Conference on Current Measurement Technology, 2005*. 152–156. IEEE.
- Sanford, Thomas, James Price, and James Girton. 2011. "Upper-Ocean Response to Hurricane Frances (2004) Observed by Profiling EM-APEX Floats." *Journal of Physical Oceanography* 41 (6): 1041–1056.
- SPACE X. 2015. *GRID FINS*. <https://www.spacex.com/news/2015/08/31/grid-fins>. (Accessed on 12/30/2019).
- Statscewich, Hank, Tom Weingartner, Seth Danielsen, Bruno Grunau, Greg Egan, and Jeb Timm. 2011. "A High-Latitude Modular Autonomous Power, Control, and Communication System for Application to High-Frequency Surface Current Mapping Radars." *Marine Technology Society Journal* 45 (3): 59–68.
- Stein, Joshua, William Holmgren, Jessica Forbess, and Clifford Hansen. 2016. "PVLIB: Open Source Photovoltaic Performance Modeling Functions for Matlab and Python." In *2016 IEEE 43rd Photovoltaic Specialists Conference (PVSC)*, 3425–3430. IEEE.
- The Associated Press. 2018. "Company Seeks to Dismantle Alaska Oil Terminal Next Year." (Accessed on 12/27/2019), *The Seattle Times*.

- UCSD. 2019. *Argo - Part of the Integrated Global Observation Strategy*. <http://www.argo.ucsd.edu/>. (Accessed on 12/30/2019).
- Ullal, Harin. 2008. *Overview and Challenges of Thin Film Solar Electric Technologies*. Technical report. National Renewable Energy Lab (NREL), Golden, CO (United States).
- Wang, K., L. Cheng, Z. Pan, and Q. Sun. 2015. "Modeling and Optimization of a Portable Hybrid Power System for the Dismounted Soldier." In *Energy and Environment: Proceedings of the 2014 International Conference on Energy and Environment (ICEE 2014), June 26-27, Beijing, China*, 3:115. CRC Press.
- Wang, Taiping, and Zhaoqing Yang. 2020. "A Tidal Hydrodynamic Model for Cook Inlet, Alaska to Support Tidal Energy Resource Characterization." *Journal of Marine Science and Engineering* 8:254.
- Webb, Douglas, Paul Simonetti, and Clayton Jones. 2001. "SLOCUM: An Underwater Glider Propelled by Environmental Energy." *IEEE Journal of Oceanic Engineering* 26 (4): 447–452.
- Wu, Shuang, Yanjun Liu, and Qi An. 2018. "Hydrodynamic Analysis of a Marine Current Energy Converter for Profiling Floats." *Energies* 11 (9): 2218.
- Xia, Qingchao, Yanhu Chen, Yujia Zang, Xin Shan, Canjun Yang, and Zhifeng Zhang. 2017. "Ocean Profiler Power System Driven by Temperature Difference Energy." In *OCEANS 2017 - Anchorage*, 1–6. IEEE.
- Xing, Xiao-Gang, Herve Claustre, Emmanuel Boss, and Fei Chai. 2018. "Toward Deeper Development of Biogeochemical-Argo Floats." *Atmospheric and Oceanic Science Letters* 11 (3): 287–290.

Appendix A – Use Case Locations

Use cases 1-4 are sited in two regions - the North Pacific and North Atlantic oceans. Inland waters are chosen for the coastal weather buoy and HF radar applications, while remaining locations are open ocean. Maps of the local regions are shown in Fig. A.1 and Fig. A.2.



Figure A.1. Locations of use cases #1 and 2.

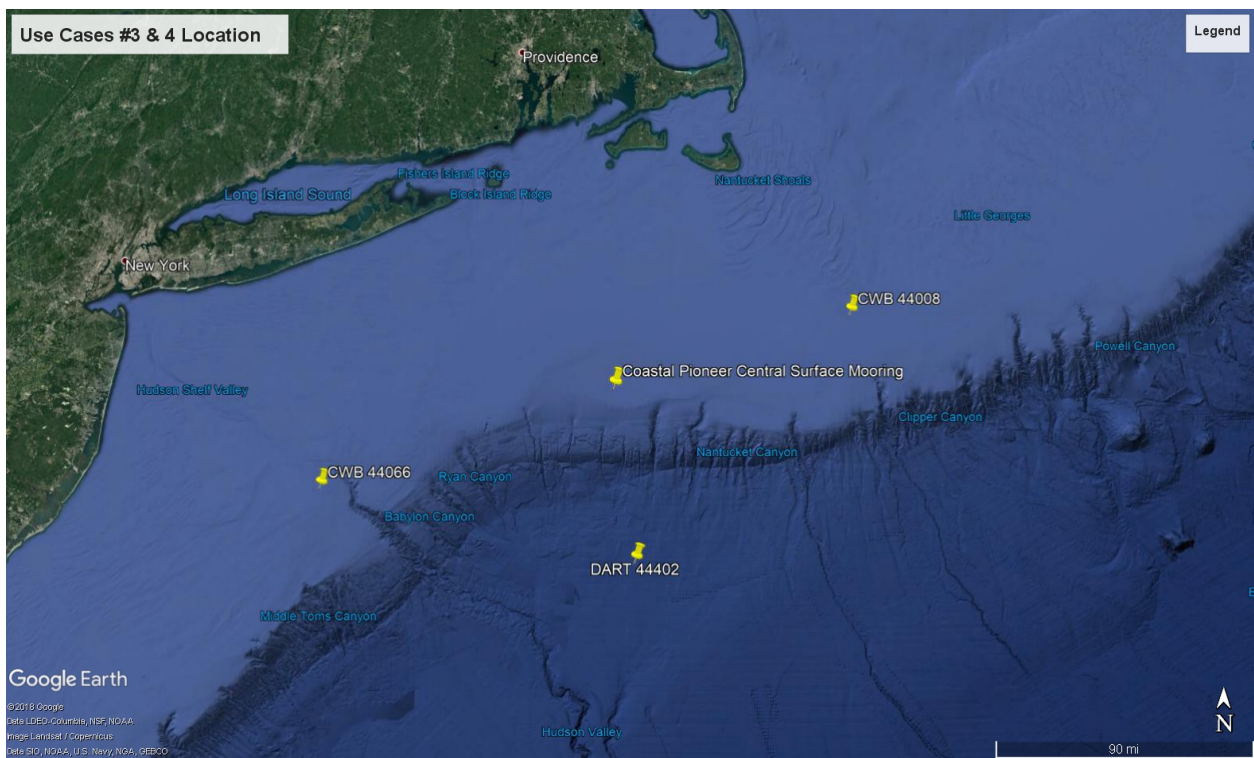


Figure A.2. Locations of use cases #3 and 4.

Appendix B – Resource Characterization Methods

B.1 Wave Power Estimation

Coastal weather buoys operated by NDBC and surface moorings operated under the National Science Foundation (NSF) Ocean Observatories Initiative (OOI) are equipped with inertial motion and positioning sensors used to quantify the sea state over time. Both report key spectral quantities needed for assessing wave energy potential: significant wave height, H_S (average height of the highest one-third of waves) and dominant or peak period, T_P . The buoys report these quantities hourly, derived from records of motion over a 5 or 20 minute sampling period. For irregular waves in deep water, a good assumption for the studied locations (all depths greater than 140 m, average periods longer than 5 s) power per unit crest length (J) is generally calculated as

$$J = \rho g^2 \frac{T_E H_S^2}{64\pi}, \quad (\text{B.1})$$

using T_E , the energy period of the waves, and is expressed in units of W/m. T_E is a statistical quantity that represents the center of the spectral distribution of wave power (Lenee-Bluhm, Paasch, and Özkan-Haller 2011). T_E can be estimated from T_P by assuming the statistical distribution of waves may be approximated by the Bretschneider spectrum (Cahill and Lewis 2014) such that,

$$T_E = 0.85T_P. \quad (\text{B.2})$$

Wave directionality, though critical for the function of several archetypes of WECs, is not important for point absorber types, the variant herein considered. Available wave energy resource may best be shown as a bivariate distribution of wave height and period in terms of the percent of time a given sea state occurs and the percentage of the total yearly energy a given sea state contains. Additional computed parameters include average yearly resource intensity (J) and an estimate of output of a suitable device for each location.

Performance of a WEC can be estimated with first-order accuracy by assuming its conversion efficiency between incoming wave energy and mechanical absorption (capture width) over a characteristic dimension is constant across sea states. However, efficiency is not constant across device scale, and can be estimated using an empirically-derived relationship with characteristic dimension (e.g., diameter for a heaving point absorber) (Babarit 2015). Using this efficiency (η) for a chosen dimension (B), WEC power (P_W) may be estimated as,

$$P_W = \eta(B)BJ \quad (\text{B.3})$$

in units of Watts (W). Efficiency as a percentage for heaving point absorber devices is determined as,

$$\eta = 1.3B + 5.6, \quad (\text{B.4})$$

an empirical relationship derived from many reported modeling and testing studies (Babarit 2015). Note this method ignores device hydrodynamics and power take-off characteristics and is thus not fully representative of the dynamics of WECs. Yearly average J at sites where it is viable is presented in units of W/m.

B.2 Tidal and Ocean Current Power Estimation

The potential for tidal power is greatest in narrow constrictions between large bodies of water experiencing tidal exchange or in large basins whose size and shape result in tidal resonance.

Ocean currents such as the Gulf Stream are swift enough to consider for power generation. Power in flow for a marine (or any) current turbine (P_T) is determined by,

$$P_T = \frac{1}{2}\rho AC_P u^3, \quad (\text{B.5})$$

where ρ is water density, A is device projected area, C_P is the coefficient of performance (kinetic energy conversion efficiency), and u is the undisturbed free-stream water velocity upstream of a device. Given the cubic relationship, power output is therefore most sensitive to velocity, and the majority of marine current energy technology development has focused on locations with flows greater than 2 m/s for commercial viability in powering an electrical grid. Many turbines will not start rotating until a minimum cut-in speed is reached, typically between 0.8-1.5 m/s.

Suitable locations are not widespread and are uncommon in the open ocean. However, Cook Inlet and the Gulf of Alaska, two of the locations selected for use cases, contain some of the best known locations for tidal energy extraction in the U.S. (Wang and Yang 2020). Tidal currents were evaluated for the region using a Finite Volume Coastal Ocean Model (FVCOM) simulation over many tidal cycles and queried at nodes closest to desired locations. Where available, as in the cases using data from an OOI surface mooring, direct measurements of current are employed. Yearly average resource intensity (kinetic power density) at sites where it is viable is presented in units of W/m^2 .

B.3 Wind Power Estimation

Estimating the wind resource and power output utilizes the same fundamental physics of flow and energy conversion as marine current energy. Direct measurements of wind speed and direction are available at the locations of each use case. The resource is evaluated in terms of kinetic power density in units of W/m^2 . Additionally, it is assumed that turbines are capable of passively or actively yawing to face the direction of flow or are of a design that does not require yaw adjustment. Hypothetical wind turbine output is reported, except for the cases using OOI data, as this surface mooring is equipped with two wind turbines and estimation of actual output is possible.

B.4 Solar Power Estimation

Solar photovoltaic (PV) power is currently used to recharge the batteries of some ocean observation platforms, including two of the assets studied. Its low cost, simplicity, and high reliability make it the first logical option for *in-situ* power generation at sea where a surface presence is allowed or feasible. Systems must invariably be paired with an energy storage mechanism in order for PV to overcome the daily cycle and stochastic cloud coverage.

The use cases utilizing NDBC weather buoy data do not benefit from direct measurement of solar irradiance. For these, we estimate the resource potential and power output using existing open-source simulation resources available through NREL: the PVWatts calculator (Dobos 2014). The software takes input in the form of location and system information and returns aggregate and time-series data with hour resolution over a ‘typical’ simulated year from the National Solar Radiation Database. The database includes nodes close to the locations for three use cases; the tsunami detection and AUV recharge cases were too far offshore. For cases where PV is already utilized, specifications of the installed hardware inform simulation. In each case a ‘standard’ module and array type is selected with the same system loss of 14% applied throughout. As for other resources, we report intensity in W/m^2 as well as a time-series showing estimated system output.

The OOI Coastal Pioneer surface mooring (location of tsunami and AUV case) benefits from solar irradiance measurements, which are used to evaluate PV potential. A pyranometer on the buoy mast measures net shortwave and longwave irradiance in units of W/m^2 with minute-scale resolution. Treating net shortwave irradiance as global horizontal irradiance (GHI), empirical fitting methods using solar zenith angle and barometric pressure may be used to estimate direct normal irradiance (DNI) and subsequently direct horizontal irradiance (DHI). This is accomplished with an open source toolbox provided by Sandia National Laboratories - PVLIB (Stein et al. 2016). These parameters, along with dew point temperature, air temperature, wind speed, and wind direction are then input into NREL's System Advisor Model (SAM) with known system parameters to simulate resource intensity and panel output consistent with PVWatts (Gilman 2015).

Pacific Northwest National Laboratory

902 Battelle Boulevard
P.O. Box 999
Richland, WA 99352
1-888-375-PNNL (7675)

www.pnnl.gov